Renewable and Sustainable Energy Reviews 155 (2022) 111861

Contents lists available at ScienceDirect

Renewable and Sustainable Energy Reviews

journal homepage: www.elsevier.com/locate/rser

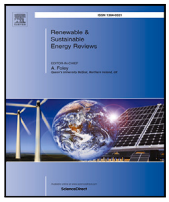

Coordinated stochastic optimal energy management of grid-connected microgrids considering demand response, plug-in hybrid electric vehicles, and smart transformers

S. Gupta [a], A. Maulik [b,*], D. Das [a], A. Singh [b]

[a] Indian Institute of Technology Kharagpur, West Bengal 721302, India
[b] Indian Institute of Technology (BHU) Varanasi, Uttar Pradesh 221005, India

ARTICLE INFO

Keywords:
Demand response
Economic load dispatch
Uncertainty model
Plug-in hybrid electric vehicle
Smart transformer

ABSTRACT

A microgrid comprises renewable and non-renewable power generating sources, controllable loads, energy storage devices and works as a single controllable entity. A gradual shift from conventional internal combustion engine-based vehicles to electric/hybrid electric vehicles has also led to a new load type in the power system. Moreover, demand-side management measures like demand response programs have become popular. This work deals with the optimal coordinated operation of a grid-connected AC microgrid consisting of controllable and uncontrollable power sources, battery storage units, considering plug-in hybrid electric vehicles and demand response programs. Stochastic models of renewable power sources, electric load demand, loads of hybrid electric vehicles (with battery charging characteristic), and grid power price are fed into "Hong's 2 m point estimate method" embedded optimal operating strategy. The objective is to minimize the cost of operation subject to the satisfaction of technical constraints. A nested stochastic optimization algorithm is implemented to find optimal generation schedule, battery dispatch strategy, and the best incentive value for an incentive-based demand response program. Different charging strategies of hybrid electric vehicles are studied, and their impacts on system operation are investigated. The optimal coordination between a voltage control scheme using a smart transformer with the energy management scheme is also investigated. Simulation studies on a thirty-three bus test system prove the efficacy of the proposed algorithm. The proposed coordinated optimal operating strategy reduces the operating cost by 17.53% ~ 17.74%. The system loss also reduces by 29.49% ~ 31.36%.

1. Introduction

The aging centralized energy infrastructure is vulnerable to the increasing power demand. Construction of new transmission facilities requires a heavy deployment of capital and is difficult due to space constraints. As a consequence, engineers proposed innovative solutions as alleviatory measures. On the generation side, engineers suggested the integration of small-scale generation sources at the customer-site ("distributed generation" (DG) in power system parlance), thereby countering the need for an expansion in the centralized generating and transmission infrastructure [1]. Uncoordinated controls of multiple generating units can cause various technical problems. Therefore, a coordinated control strategy for several generating units in a given control area was proposed, which led to the evolution of the microgrid concept. A microgrid comprises a medium voltage or low voltage distribution network with multiple energy sources (both controllable and uncontrollable), energy storage devices, controllable loads, operating as a single controllable entity, either working in tandem with the main-grid (grid-connected operation) or isolatedly (autonomous/island operation) [2].

On the load side, customers receive incentives to cooperate with the utilities. Customers shift or reduce their demands during peak periods to ensure grid reliability, from which the concept of demand response (DR) arose. According to the United States Department of Energy (DOE), DR is the modification of consumer's demand for energy through various methods such as financial incentives and behavioral change through education [3]. There are broadly two kinds of demand response programs: price-based (PBDR) and incentive-based (IBDR). PBDR passes the variations in the wholesale market to the retail market so that customers can pay for the actual value of electricity. It helps in reducing price volatility. For instance, in the Time of Use (TOU) scheme, the price is different at different times of the day. IBDR, on the other hand, encourages customers to regulate their consumption

* Corresponding author.
E-mail address: avirupmaulik.eee@itbhu.ac.in (A. Maulik).

https://doi.org/10.1016/j.rser.2021.111861
Received 24 June 2021; Received in revised form 23 September 2021; Accepted 31 October 2021
Available online 24 November 2021

Nomenclature

$f_i(x_i)$	pdf of ith uncertain input variable x_i
$p_i(x_{is})$	Probability of input variable at state s
x_{is}	Input variable at state s
$x_{il/iu}$	Lower/upper bound of input variable at state s
$f_w(v)$	Weibull distribution as a function of wind speed v
k	Shape factor of Weibull pdf
c	Scale factor of Weibull pdf
$\Gamma(.)$	Gamma function
μ_v	Mean of wind speed
$\eta_{chg/dis}$	Charging/discharging efficiency of BESS
$EBAT^{min/max}$	Minimum/maximum battery energy specification
PB^{rated}	Rated battery power
P_{grid}^{max}	Maximum active power handling capacity of LSC of ST
$IT/ITMAX$	Iteration count/maximum iteration of PSO
$NPOP$	Population size/number of variables in PSO
$NVARS$	Number of control variables in the PSO algorithm
$pos/pos^+/pos^-$	Position/Upper limit/Lower limit of control variable in PSO
vel/WT	Velocity/weight in the PSO algorithm
$rand()$	Random number
σ_v	Standard deviation of wind speed
ε/A	Demand price elasticity/Constant in PBDR
$\nu_j(t)/r_j^{PBDR,P}$	Binary decision/Load demand response rate of PBDR on price level j during period t
$LDU_i(.)$	Uncertain portion of predicted load demand
$\rho_{cj}(t)$	Electricity price for customers on price level j at hour t
$\rho_{0c}(t)$	Original Electricity price for customers without PBDR at hour t
Ω_J	Set of PBDR price levels
PW_s	Power output of wind turbine at state s
v_s	Wind speed at state s
v_{ci}	Cut-in wind speed
v_{co}	Cut-out wind speed
v_r	Rated wind speed
PW_r	Power rating of wind turbine
$f_s(S)$	Beta distribution as a function of solar irradiation S
α, β	Shape factors of beta pdf
μ_s	Mean of solar irradiation
σ_s	Standard deviation of solar irradiation
PS_s	Power output of solar power generator for state s
T_{cell}	PV cell temperature in Celsius
T_{amb}	Ambient temperature in Celsius
T_{nom}	Normal operating cell temperature in Celsius
S_s	Solar irradiation at state s
I_{PV}	PV cell current at s
I_{SC}	Short circuit current
K_i	Current temperature coefficient
V_{PV}	PV cell voltage at s
V_{OC}	Open circuit voltage
K_v	Voltage temperature coefficient
V_{MPP}	Voltage at maximum power point
I_{MPP}	Current at maximum power point
N	Number of cells in PV array
$f_L(l)$	Normal distribution as a function of load l
μ_l	Mean of load
σ_l	Standard deviation of load
$f_d(d)$	Log-normal distribution as a function of daily driven distance d
μ_m	Mean of daily driven distance
σ_m	Standard deviation of daily driven distance
D_{max}	All electric range of PHEV
μ_m, σ_m	Mean and standard deviation of log-normal pdf
t_{st}	Start time of PHEV charging
$f_{ch}(.)$	pdf of charging pattern
$f_{price}(K_{grid})$	Normal distribution as a function of grid energy price K_{grid}
μ_{price}	Mean of grid energy price
σ_{price}	Standard deviation of grid energy price
Z	Vector of stochastic output variable
$p_{l,k}$	Location of kth concentration for lth input random variable
$w_{l,k}$	Weight of kth concentration for lth input random variable
μ_{pi}	Mean of ith input stochastic variable
$M_3(pl)$	Third central moment of pl
μ_{pl}	Mean of pl
$\lambda_{l,3}$	Coefficient of skewness
m	Number of input random variables
$\xi_{l,k}$	Standard location
$V_{max/min}^{GC}$	Maximum/minimum allowed voltage in a network as per grid code
V_{STMV}^*	Smart transformer voltage set point on microgrid side
Ω_t	Set of all times (hour) in a day
$E(.)$	Expected value
$P_{CHEV}(.)$	Active power fed to EV charger
$PL_i^{DR}(.)$	Load at bus i participating in DR program
$PL_i^0(.)$	Original demand at bus i
η	Percentage of load participating in DR program
$El(t,t)$	Self elasticity
$El(t,h)$	Cross elasticity
$\rho(t)$	Spot electricity market price at time t
$\rho_0(t)$	Initial electricity market price at time t
$I(t)$	Incentive offered per unit of load curtailed or shifted at time t for participating in IBDR
$PL_i(.)$	Modified load at bus i after implementation of DR
$\Delta PL_i(.)$	Change in load at bus i after implementation of DR

by offering them incentives. One example of IBDR is peak time rebate (PTR), in which consumers are tendered incentives during the peak duration to shift or curtail their non-critical loads. Consumers pay electricity bills at a flat tariff without knowing the actual market conditions in the conventional power market. IBDR gives them a choice to understand it and actively participate in it.

$g_{l,k,t}$	Set of power system state variables (voltage magnitude, phase angle, line current
$TOC(t)$	Total operating cost at time t
$x(t)$	Control variables
Ω_x	Set of control variables
$PG_i(t)$	Active power generation of ith dispatchable unit at time t
$PB(t)$	BESS charging power at time t
$P_{grid}(.)$	Power imported from main grid/sub-station
Ω_B	Set of system buses
Ω_G	Set of all dispatchable units
a_j, b_j, c_j	Fuel cost coefficients of dispatchable unit j
$PW_i(.)$	Active power injection from wind DG at bus i
$PS_i(.)$	Active power injection from solar DG at bus i
$QW_i(.)$	Reactive power injection from wind DG at bus i
$QS_i(.)$	Reactive power injection from solar DG
$QG_i(.)$	Reactive power injection from dispatchable DG at bus i
$QL_i(.)$	Reactive power load at bus i
$QB_i(.)$	Reactive power fed to battery converter at bus i
$Q_{grid}(.)$	Reactive power injection from grid
$Q_{CHEV_i}(.)$	Reactive power fed to EV charger at bus i
$V_i(.)$	Voltage magnitude at bus i
$\delta_i(.)$	voltage phase angle i
θ_{ij}	Angle of ijth element of Y-bus
$PG_i^{min/max}$	Minimum/maximum active power handling capacity of unit i
$QG_i^{min/max}$	Minimum/maximum reactive power handling capacity of unit i
Ω_{ln}	Set of all lines in the system
I_{ln}^{max}	Maximum line rating
$I_{ln(.)}$	Line current
$EBAT(.)$	Energy of the battery
σ_{pl}	Standard deviation of pl

Acronym

DG	Distributed Generation
DR	Demand Response
$PBDR$	Price-based demand response
$IBDR$	Incentive-based demand response
TOU	Time of Use
PTR	Peak time rebate
IC	Internal combustion
$PHEV$	Plug-in Electric Vehicle
RTP	Real time pricing
EV	Electric Vehicle
ADR	Automated demand response
$V2G$	Vehicle to grid
PV	Photovoltaic
$HEMS$	Home energy management system
DSM	Demand side management
I/C	Interruptible/Curtailable
DRP	Demand Response Program
DER	Distributed energy resource
$VRES$	Variable renewable energy sources
$BESS$	Battery energy storage system
CPP	Critical peak pricing
ST	Smart transformer
PEM	Point Estimate Method
pdf	Probability distribution function
RT	Real Time
WPG	Wind power generation
PEM	Point Estimate Method
MV	Medium voltage
HV	High Voltage
PQ	Power quality
GSC	Grid side converter
LSC	Load side converter
VRM	Voltage rise margin
VDM	Voltage drop margin
PI	Performance indicators
AVD	Average voltage deviation
PSO	Particle Swarm Optimization
NGT	Natural Gas Turbine
FF	Fill factor
SOC	State of charge

Further, with growing environmental concerns across the globe, conventional internal combustion (IC) based vehicles are increasingly being replaced by plug-in electric/plug-in hybrid electric vehicles (PHEV). The presence of the PHEVs introduces a new type of load demand. The charging load of PHEVs alters the load demand curve. During certain hours in a day, the additional charging load may lead to feeder and transformer overloads, increased network loss, and system-wide voltage dips. Therefore, it is essential to study the impact of PHEV charging load in a modern power system to find innovative operating strategies to cater to the system demand without stressing the existing electrical infrastructure [4].

1.1. Literature review

Aliasghari et al. used a stochastic model and increased the profits of the microgrid operator by synchronizing the use of DGs and BESS [5]. Also, the authors used a TOU-based DR program for EV owners. However, schedules of battery and dispatchable units were not optimized [5]. Yang et al. proposed an RTP-based DR to minimize electricity purchase and maximize renewables utilization for a home energy management system (HEMS) with renewables, storage devices, and PHEVs [6]. Gazijahani and Salehi proposed a two-stage scheme to reduce the cost of operation and enhance reliability [7]. The authors carried out simultaneous optimal scheduling of DERs and allocation of section switches in the first stage to improve the reliability. A critical peak pricing DR program is implemented in the next stage to flatten the load profile and reduce the investment cost [7]. Some researchers have discussed and prioritized different types of DR programs. Imani et al. ranked various DR programs based on the achievement of objectives like peak reduction, cost reduction, peak shaving by using a stochastic model of renewables [3]. Noor et al. used block-chain technology in the demand-side management (DSM) framework to schedule the loads under supply-side constraints. However, they have not incorporated DG in their network and followed a deterministic model for the load [8]. Müller and Möst explored DR potential in the present and futuristic power system framework. However, the authors used a deterministic approach in the study [9]. Nan et al. optimized the power schedule for a residential community using price-based DR considering mainly interruptible loads [10]. However, the authors did not consider the

uncertainties associated with load or solar DG. Pfeifer et al. considered interconnected islands with renewable power sources, vehicle to grid (V2G) operation of EVs, and storage technology for analyzing their synergy [11]. However, the authors did not account for the uncertainties of RES. Also, the authors did not consider a demand response program but investigated a demand response technology (EVs).

Many researchers also studied incentive based DR program such as interruptible/curtailable (I/C) [12,13]. Authors in [12] modeled uncertainties of renewable power and simultaneously implemented DR and network reconfiguration to minimize the operating cost. Imani et al. carried out a sensitivity analysis of incentive and penalty for an Interruptible/Curtailable (I/C) DRP [13]. The authors studied the effect on operating cost, profits, and peak shaving in their paper [13].

Biroon et al. investigated power quality issues (including voltage deviation) of integrating EV and Distributed energy resource (DER) with a constant tariff [14]. The researchers proposed a modified tariff structure to mitigate the mentioned issues. However, the authors did not consider the generation, load, and price uncertainties in the model [14]. Zhou et al. ensured the security of energy trading in an EV-based incentive-compatible DR framework by using blockchain technology [15]. Monfared et al. used a hybrid of TOU and RTP scheme for DR optimization in a stochastic framework for day-ahead scheduling of a microgrid [16]. The authors had also considered uncertainties of control variables and generator parameters. Good studied and incorporated consumer's preferences and biases in the demand response model in a deterministic framework [17]. Khalili et al. studied the impact of various battery technologies on the cost of operation under an IBDR framework [18]. Eseye et al. maximized the utility's profit by coordinating EVs, variable renewable energy sources (VRES), and BESS in a stochastic framework [19]. However, the authors did not optimize the incentive offered to the consumers, uncertainties, and scheduling of dispatchable generating units. Li and Li considered a real-time pricing regime and carried out a two-level optimization to minimize the net operating cost in an islanded microgrid. Also, the researchers investigated the integration of EV charging stations and their deployment as a demand response tool [20]. The authors, however, did not incorporate renewable and load uncertainties in the model. Sadeghian et al. improved the reliability of a radial distribution system by implementing a combination of price-based DR and smart scheduling of EVs [21]. However, renewable sources, and uncertainties were not considered in this work.

Iwafune et al. used a combination of the Markov chain model and Monte Carlo simulation to model the EV driving pattern [22]. The authors suggested controlling the charging and discharging pattern of EV batteries in a TOU tariff regime for economic benefits [22]. Uncertainties due to load and solar PV were not considered in [22]. Ren et al. used RTP and offered a reward to EV owners for discharging and a penalty for charging during peak hours [23]. The researchers also considered EV owner's satisfaction in the scheduling strategy of the EV aggregator. Gao et al. minimized the charging/discharging cost of EVs and load fluctuation considering EV owner's willingness using ADR [24]. Wang et al. scheduled EV charging/discharging using multi-price scales and reduced load uncertainty by comprehensive demand [25]. Yusuf et al. proposed V2G operation during foreseen critical events in conjunction with a critical peak pricing (CPP) DR program to minimize the cost associated with PEV activities [26].

Conventional IC engine-based vehicles are making way for EVs/PHEVs all over the world. Therefore, it is imperative to model the charging load of EVs/PHEVs for proper planning and operation of a distribution network. Investigations on the modeling of PHEV load and impact assessment have been reported in the literature over the last few years. Qian et al. proposed a method of stochastic modeling of EV/PHEV load in a distribution network [27]. Shaaban et al. reported a method to assess the energy consumption of PHEVs [28]. The authors used the model to study the impact of PHEVs on the distribution network and allocated distributed generation (DG) optimally. Stochastic optimal scheduling and DR implementation were not a part of the study. Mu et al. used a "spatio-temporal model" to characterize the behavior of EV charging load, and used a combination of "Monte-Carlo simulation" (MCS) and sequential power flow to investigate the impact on the grid [29]. However, renewable uncertainties, load demand, optimal scheduling, and DR were not included in the study. Honarmand et al. considered a smart microgrid containing dispatchable and non-dispatchable power sources and an EV parking lot [30]. The authors proposed a deterministic scheduling algorithm for the system [30]. However, the authors did not consider uncertainties and DR in the scheduling strategy. Rostami et al. presented stochastic models of EV charging strategies and carried out distribution network reconfiguration to minimize the operating cost [31]. However, the authors did not include renewable and load uncertainties or DR in the paper. Yao et al. reported a real-time charging strategy for an EV parking lot [32]. However, the researchers did not consider stochastic scheduling of distributed generation units and DR in this study. Kamankesh et al. suggested a scheduling algorithm for dispatchable sources and storage units considering stochastic models of PHEV charging load [33]. However, the authors did not consider renewable and grid price uncertainty or DR in their model. Chaudhari et al. used a hybrid optimization scheme to schedule charging of energy storage units in a PV integrated EV parking lot [34]. However, the authors carried out the scheduling in a deterministic framework. Further, the authors did not consider DR and dispatchable unit scheduling in the study. Rahmani et al. proposed an "adaptive model predictive control" approach for managing the charging of PEVs to minimize the cost in a stochastic framework [35]. However, the authors did not consider the dispatchable unit scheduling and DR in this paper. Quddus et al. proposed an approach for energy exchange between PEV charging stations, commercial buildings, and the power grid for reducing the operating cost [36]. MCS was used for modeling EV uncertainty, although DR was not considered in the study. Moghaddas et al. used "information gap decision theory" IGDT) to model EV demand uncertainty in [37]. The authors formulated objective functions for reducing the operating cost using "risk-neutral", and "Robustness and opportunity" approaches. However, the authors did not include DR in this study. Emrani et al. adopted MCS to model uncertainties of renewable sources, price, and EV while minimizing the cost of a residential energy hub [38]. Ahrabi et al. adopted a hybrid IGDT-stochastic approach for modeling uncertainties while minimizing the operating cost in a distribution network [39]. The uncertainties of EV were modeled using a stochastic approach, while the authors used an IGDT approach for modeling wind generation uncertainty.

Lan et al. reported an energy management strategy of a renewable MG comprising wind and solar DGs, BESS, and PHEVs [40]. Energy demands of PHEVs were modeled using a support vector machine-based machine learning approach. The objective was to minimize the operating cost. A modified dragonfly algorithm was used for solving the optimization problem. The authors had also considered network reconfiguration in the formulation. However, the authors had not considered uncertainties associated with renewable generation, load demand, and grid energy price. The authors had also not incorporated dispatchable sources and the use of STs in the formulation. Flexible loads were modeled in the formulation. However, the DRP was not an IBDRP. Wang et al. proposed data-driven stochastic energy management for an AC/DC hybrid MG consisting of PHEVs, renewable generation, and loads [25]. Uncertainty modeling was done using a combination of support vector machine and Hong's $2m + 1$ PEM. Network reconfiguration was also carried out to reduce the operating cost. However, DRP and the use of STs were not explored in the paper. Mohamed et al. proposed a multi-agent-based energy management strategy for a smart island to reduce the operating cost [41]. The authors considered an energy hub and multi-microgrid exchanging power based on peer-to-peer trading. The energy hub comprises multiple energy vectors like wind energy, tidal energy, solar energy, and thermal power. However, the authors had not explored DRP, network reconfiguration, and STs. Ma et al.

suggested a two-stage risk-constrained energy scheduling approach for an active distribution network [42]. The authors minimized cost and risk by using particle swarm optimization. However, the authors had not considered PHEVs, STs, and IBDR in this paper. Mohamed et al. used fuzzy cloud theory in conjunction with stochastic modeling of renewable generation and PHEV loads in [43]. The objective was to minimize the operating cost by optimally scheduling BESS and generation sources in a fuzzy stochastic framework. However, the authors had not considered DRP, network reconfiguration, and STs in the problem. Li et al. proposed a bi-level energy management scheme for a community-integrated energy system and an EV charging station for energy cost minimization [44]. The energy cost of the energy system was minimized at the upper level, and the EV charging cost was minimized at the lower level. However, the authors did not consider network reconfiguration, incentive cost optimization, and STs in the formulation. Alfaverh et al. proposed a vehicle to grid (V2G), vehicle to home (V2H) based demand response approach for energy management of residential loads [45]. The authors used Q-learning and real-time pricing schemes in the paper. However, uncertainties, STs, network reconfiguration were not considered. Ghofrani and Majidi proposed the formulation of a bi-lateral contract between EV aggregator and DGs to minimize the operating cost, voltage deviation [46]. The authors also proposed optimal capacitor sizing and siting in the paper. However, the authors did not focus on dispatchable generation, network reconfiguration, and STs.

Researchers have also recently proposed the use of smart transformers (ST) to improve the performance of a distribution network [47]. An ST can mitigate power quality issues like voltage sag, harmonic compensation, voltage rise, etc. An ST can also provide ancillary service to the grid. Different voltage control strategies in a distribution network using an ST have been reported in the literature [48–53]. Some researchers have also reported investigations on using a ST for power flow control within and between microgrids [54,55], islanding operation [56], voltage and frequency support in a renewable rich microgrid [57], etc. However, studies on the control and operation of an ST have been reported in a deterministic framework. In other words, research endeavors on ST reported so far have not considered probabilistic models of renewables, loads, and PHEV. Moreover, the coordination between different operating strategies like economic scheduling of dispatchable and storage units, DR, and ST working in tandem in a stochastic framework has not been explored fully. A summary of the literature review is given in Table 1.

1.2. Contributions of the present work

Following points are observed from the literature review:

- Many researchers have reported investigations on energy management schemes of a grid-connected MG incorporating renewable generations, DRPs, BESS scheduling, and PHEV loads [3,5–25,25,26,29,30,30–46]. On the other hand, several studies on STs have also been reported. However, most studies on STs have been done without considering uncertainties of power system variables and energy management schemes [47–57]. In other words, to the best of the author's knowledge, microgrid energy management and studies of STs have been carried out separately so far.
- Incentive values in most IBDR schemes have been assumed to be pre-defined.
- The impact of a voltage control strategy using an ST on the cost and loss of a network has generally not been studied. Focuses of studies reported on voltage control by STs were mainly on voltage profile only.

A stochastic optimal operating framework for a grid-connected microgrid to reduce the operating cost is proposed in this paper. Uncertainties of renewable sources, load demand, grid energy price, Plug-in hybrid electric vehicle (PHEV) driving, and charging patterns are modeled using a stochastic approach and incorporated in the scheduling problem. The optimal operating measures include optimal scheduling of dispatchable sources, battery energy storage systems, and using an optimal IBDR. An attempt is made in this work to bridge the gap areas identified in the previous threads of the reported literature. Contributions of the present paper are as follows:

- The incentive to be offered to the customers for participating in the DR program is optimized considering different PHEV charging strategies reported in the literature.
- A method to evaluate the hourly load demand of PHEVs considering the battery charging characteristics, stochastic models of daily driven distance, and charging strategies are presented in detail and incorporated in the scheduling problem. The method proposed to evaluate the probabilistic charging demand of a PHEV has a different approach than that reported in [27] but provides similar profiles.
- The optimal coordination of smart transformer (ST) in conjunction with IBDR, ELD, and BESS is proposed to improve the system voltage profile, reduce the system operating cost, and reduce the loss.
- The impact of an optimal voltage control strategy employing an ST on the expected operating cost and system loss is studied.

1.3. Arrangement of the paper

The rest of the paper is arranged as follows. Uncertainty modeling of renewable sources, load demands, grid energy price, and PHEV are presented in Section 2. ST and PHEV load modeling are discussed in Section 3. The mathematical formulation of the problem and solution strategy are presented in Section 4. We have discussed the simulation results in Section 5, followed by conclusions in Section 6.

2. Uncertainty modeling

Stochastic models and Hong's 2 m Point Estimate Method (PEM) are discussed in this section.

2.1. Stochastic models of uncertain variables

All uncertain variables are represented by a probability density function (pdf). The pdf of the ith uncertain variable is given as $f_i(x_i)$, x_i is the uncertain input parameter. Continuous pdfs are converted to discrete states (using appropriate step size) by integrating the pdf. The probability of a state s ($\rho_i(x_{is})$) corresponding to a state (x_{is}) is found as follows [60]:

$$\begin{cases} \rho_i(x_{is}) = \int_{x_{il}}^{x_{iu}} f_i(x_i)dx_i \\ x_{is} = \frac{x_{il}+x_{iu}}{2} \end{cases} \quad (1)$$

x_{il} and x_{iu} are the lower and upper bounds of the input stochastic variable for the state s. Uncertainties of wind power, solar power, load demand, PHEV load demand, and grid power price are considered in this work.

2.1.1. Wind power generation (WPG) uncertainty

Wind power generation depends on wind speed. Wind speed is the stochastic input variable and commonly follows a “Weibull pdf” given below [60]:

$$f_w(v) = \frac{k}{c}\left(\frac{v}{c}\right)^{k-1} \exp[-(v/c)^k] \; for \; c > 1, k > 1 \quad (2)$$

where v, k, and c stand for wind speed (m/s), shape, and scale factor respectively. Shape parameter (k) and scale factor (c) are related to the mean (μ_v) and standard deviation (σ_v) of the wind speed as follows:

$$\begin{cases} k = \left(\frac{\sigma_v}{\mu_v}\right)^{-1.086} \\ c = \frac{\mu_v}{\Gamma(1+\frac{1}{k})} \end{cases} \quad (3)$$

Table 1
Summary of literature review.

Ref	Uncertainty				DR	opt BESS	ELD	ST	Objectives
	Ren	EV	Load	Price					
[5]	Yes	Yes	Yes	Yes	Yes	No	Yes	No	Min cost
[6]	Yes	NA	Yes	No(RT)	Yes	Yes	NA	No	Min elect purchase, max renewable utilization
[7]	Yes	NA	Yes	Yes	Yes	NA	Yes	No	Min investment & operation cost
[8]	NA	NA	No	No	Yes	NA	NA	No	Min cost of electricity usage & discomfort cost due to load shifting
[9]	No	NA	No	No	Yes	NA	NA	No	Quantify DR potential & study flexibility potential
[10]	No	No	No	No	Yes	Yes	Yes	No	Min power purchase cost
[11]	No	No	No	No	Yes	Yes	NA	No	Integrate islands with VRES potential
[12]	Yes	NA	No	Yes	Yes	Yes	Yes	No	Min operating cost, power loss, cost of DR; improve reliability
[13]	No	NA	No	No	Yes	Yes	Yes	No	Min operating cost
[14]	No	No	No	No	Yes	Yes	NA	No	Opt tariff structure to mitigate VD & PQ
[15]	NA	Yes	No	No	Yes	NA	NA	No	Opt economic performance under information asymmetry
[16]	Yes	NA	Yes	Yes	Yes	NA	Yes	No	Max microgrid profit
[17]	No	NA	No	No	Yes	NA	NA	No	Min cost and ensure elect and thermal comfort
[18]	Yes	NA	Yes	No	Yes	Yes	NA	No	Min annual operating cost
[19]	No(RT)	No	No(RT)	No(RT)	Yes	Yes	NA	No	Max day-ahead & real-time microgrid profit
[20]	Yes	Yes	Yes	No(RT)	Yes	Yes	Yes	No	Min operating cost of isolated microgrid & charging cost of EV
[21]	Yes	Yes	No	No(RT)	Yes	No	No	No	Opt reliability indices
[22]	No(RT)	Yes	No(RT)	No	Yes	NA	NA	No	Optimize charging & discharging of EV
[23]	NA	Yes	NA	No	Yes	NA	NA	No	Max EV aggregator's profits considering EV owner's satisfaction
[24]	NA	No	No	No	Yes	NA	NA	No	Min charging/discharging cost of EV and load fluctuation
[25]	NA	Yes	Yes	No	Yes	NA	NA	No	Max profit of power grid operators
[26]	NA	No	No	No	Yes	NA	NA	No	Min cost
[27]	NA	Yes	No	No	No	NA	NA	No	Stochastic modeling of EV
[28]	No	Yes	No	No	No	NA	No	No	Max penetration level of PEVs
[29]	NA	Yes	No	No	No	NA	NA	No	Characterize the behavior of EV charging load
[30]	No	No	No	Yes	No	NA	Yes	No	Min main grid, dispatchable DGs and EV power exchanged with microgrid
[31]	No	Yes	No	No	Yes	NA	No	No	Min cost of power imported from upstream grid, loss, switching operations
[32]	NA	No	No	No	Yes	NA	No	No	Max selected EV for charging, min total charging cost
[33]	Yes	Yes	No	No	No	Yes	Yes	No	Min operating cost of microgrid
[34]	No(RT)	No(RT)	No	No	Yes	Yes	Yes	No	Min power purchase cost, degradation cost of ESS & levelized cost of energy for PV
[35]	Yes	Yes	No	No	No	NA	NA	No	Min operating cost
[36]	Yes	Yes	No	No	Yes	NA	Yes	No	Min cost
[37]	Yes	Yes	Yes	Yes	Yes	NA	Yes	No	Max profit
[38]	Yes	Yes	No	Yes	Yes	NA	Yes	No	Min cost of a residential energy hub
[39]	Yes	Yes	No	No	Yes	NA	NA	No	Min operating cost
[47]	NA	NA	NA	NA	No	NA	NA	Yes	Study impact of ST on grid
[48]	No	No	No	No	No	No	NA	Yes	Control power transfer through PCC
[49]	No	No	No	No	No	NA	No	Yes	Voltage and line congestion control
[50]	No	No	No	NA	No	NA	NA	Yes	Voltage control
[51]	NA	NA	No	NA	No	No	NA	Yes	Voltage control
[52]	NA	NA	No	NA	No	NA	No	Yes	Impact on grid voltage power quality
[53]	No	NA	No	NA	No	NA	NA	Yes	Voltage control using 3 setpoints
[54]	NA	NA	No	No	No	NA	No	Yes	Control power exchange with main grid by controlling voltage
[55]	No	NA	No	NA	No	NA	No	Yes	Control power exchange with main grid by controlling voltage
[56]	No	NA	No	NA	No	No	NA	Yes	Enhance possibility of islanding operation within multi microgrids
[57]	No	NA	No	NA	No	No	No	Yes	Control power to control voltage & frequency
[40]^{AM}	No^{AM}	Yes^{AM}	No^{AM}	No^{AM}	Yes(ToU)^{AM}	Yes^{AM}	NA^{AM}	No^{AM}	Min cost of operation^{AM}
[58]^{AM}	Yes^{AM}	Yes^{AM}	Yes^{AM}	Yes^{AM}	Yes(ToU)^{AM}	Yes^{AM}	Yes^{AM}	No^{AM}	Min cost of operation^{AM}
[41]^{AM}	Yes^{AM}	Yes^{AM}	Yes^{AM}	Yes^{AM}	Yes(ToU)^{AM}	Yes^{AM}	Yes^{AM}	No^{AM}	Min cost of operation^{AM}
[43]^{AM}	Yes^{AM}	Yes^{AM}	No^{AM}	No^{AM}	Yes(ToU)^{AM}	Yes^{AM}	Yes^{AM}	No^{AM}	Min cost of operation^{AM}
[59]^{AM}	No^{AM}	NA^{AM}	No^{AM}	No^{AM}	No^{AM}	NA^{AM}	NA^{AM}	No^{AM}	Techno-economic assessment^{AM}
[44]^{AM}	Yes^{AM}	Yes^{AM}	No^{AM}	Yes^{AM}	Yes^{AM}	Yes^{AM}	NA^{AM}	No^{AM}	Min operating cost^{AM}
[45]^{AM}	NA^{AM}	No^{AM}	No(RT)^{AM}	No^{AM}	Yes(ToU)^{AM}	NA^{AM}	NA^{AM}	No^{AM}	Energy management through V2G and V2H^{AM}
[46]^{AM}	Yes^{AM}	Yes^{AM}	No^{AM}	No^{AM}	Yes(ToU)^{AM}	NA^{AM}	NA^{AM}	No^{AM}	Min cost of system loss, capacitor cost, penalty cost for voltage violations^{AM}

The pdf is converted to discrete states using wind speed steps of 1 m/s. The output of the wind turbine (PW_s) for the state s is found as follows:

$$PW_s(v_s) = \begin{cases} 0 & : 0 \le v_s < v_{ci}, v_s \ge v_{co} \\ PW_r \frac{v_s - v_{ci}}{v_r - v_{ci}} & : v_{ci} \le v_s < v_r \\ PW_r & : v_r \le v_s < v_{co} \end{cases} \quad (4)$$

v_{ci}, v_r, and v_{co} denote the cut-in, rated, and cut-out speed respectively. PW_r is the rating of the WPG.

2.1.2. Solar power generation

The input stochastic variable is solar irradiation (S, kW/m^2). Solar irradiation pdf follows "Beta" distribution [60] as shown below:

$$f_s(S) = \frac{\Gamma(\alpha+\beta)}{\Gamma(\alpha)\Gamma(\beta)}(S)^{\alpha-1}(1-S)^{\beta-1} \quad : \alpha, \beta > 0 \quad (5)$$

α and β are the shape factors, related to the mean (μ_S) and standard deviation (σ_S) as detailed below:

$$\begin{cases} \beta = (1-\mu_s)(\frac{\mu_s(1+\mu_s)}{\sigma_s^2} - 1) \\ \alpha = \frac{\mu_s \beta}{1-\mu_s} \end{cases} \quad (6)$$

The discretization of pdf is carried out by taking a step size of 0.1 kW/m^2. The power output of the solar power generator for state s (PS_s) is found as [60]:

$$\begin{cases} T_{cell} = T_{amb} + \frac{S_s(T_{nom}-20)}{0.8} \\ I_{PV} = s[I_{SC} + K_i(T_{cell} - 25)] \\ V_{PV} = V_{OC} - K_v T_{cell} \\ FF = \frac{V_{MPP} I_{MPP}}{V_{OC} I_{SC}} \\ PS_s(s) = N \times FF \times V_{PV} \times I_{PV} \end{cases} \quad (7)$$

T_{cell}, T_{amb}, and T_{nom} are the cell, ambient, and nominal temperatures in °C. I_{PV} is the cell current, while V_{PV} is the cell voltage. I_{SC} is the short circuit current, and V_{OC} is the open-circuit voltage. V_{MPP} and I_{MPP} denote the voltage and current, respectively, for maximum power point condition. FF denotes the fill factor, while PS_s is the power output of the SPV array for the state s. The array comprises N number of cells. The voltage temperature coefficient ($V/°C$) and the current temperature coefficient ($A/°C$) are denoted by K_v and K_i respectively.

.

2.1.3. Load demand

The load demand uncertainty follows a normal distribution given below [60]:

$$f_L(l) = \frac{1}{\sigma_1\sqrt{2\pi}} exp[-(\frac{l-\mu_l}{\sqrt{2}\sigma_l})^2] \quad (8)$$

The mean and standard deviation are denoted by μ_l and σ_l, respectively. The continuous pdf is discretized to seven discrete states varying from $\mu_l - 3\sigma_l$ to $\mu_l - 3\sigma_l$ in steps of σ_l.

2.1.4. Plug-in hybrid electric vehicle

The charging energy requirement of a PHEV depends on the daily driven distance (d). The daily driven distance is modeled using a log-normal distribution [27,31]:

$$f_d(d) = \frac{1}{\sigma_d d\sqrt{2\pi}} exp[-(\frac{ln(d)-\mu_d}{\sqrt{2}\sigma_d})^2] \tag{9}$$

The mean and standard deviation of the log-normal distribution are μ_d and σ_d. μ_d and σ_d are calculated from the mean (μ_m) and standard deviation (σ_m) using the following relationship:

$$\begin{cases} \mu_d = ln(\frac{\mu_m^2}{\sqrt{\mu_m^2+\sigma_m^2}}) \\ \sigma_d = \sqrt{ln(1+\frac{\sigma_m^2}{\mu_m^2})} \end{cases} \tag{10}$$

The pdf of the daily driven distance is discretized in steps of 1 mile. The state of charge (SOC) of the PHEV battery corresponding to a daily driven distance of d_s at the beginning of the charging period is $SOC_s(d_s)$[31]:

$$SOC_s(d_s) = (1-\frac{d_s}{D_{max}}) \times 100 \tag{11}$$

D_{max} is the all electric range of the PHEV. Three different charging strategies are considered in this work. They are as follows:

- **Uncoordinated charging:** A uniformly distributed pdf describes the charging pattern for an uncoordinated charging strategy [31]:

$$f_{ch}(t_{st}) = 1 \quad : 18 \le t_{st} \le 19 \tag{12}$$

  t_{st} is the start time of the charging process.
- **Coordinated charging strategy:** The uncoordinated charging strategy is modeled using a uniformly distributed pdf as given below [31]:

$$f_{ch}(t_{st}) = \frac{1}{3} \quad : 21 \le t_{st} \le 24 \tag{13}$$

- **Smart charging strategy:** The smart charging strategy is modeled using a normal pdf as shown below [31]:

$$f_{ch}(t_{st}) = \frac{1}{3\sqrt{2\pi}} exp[-(\frac{t_{st}-1}{4.243})^2] \tag{14}$$

The pdf of daily driven distance, battery charging characteristic, and the pdf of charging strategy are combined to evaluate the charging load of PHEV for every hour.

2.1.5. Grid energy price

The grid energy price uncertainty is modeled using a normal pdf [60]:

$$f_{price}(K_{grid}) = \frac{1}{\sigma_{price}\sqrt{2\pi}} exp[-(\frac{K_{grid}-\mu_{price}}{\sqrt{2}\sigma_{price}})^2] \tag{15}$$

K_{grid} is the grid energy price. The mean and standard deviation are denoted by μ_{price} and σ_{price} respectively. The continuous normal pdf is discretized into seven states, as discussed in Section 2.1.3.

2.2. Hong's 2 m point estimate method

Several approaches to handle power system uncertainties have been reported in the literature. Methods can be probabilistic, possibilistic, information gap decision theory, robust optimization, copula theory, etc. Uncertainties of renewable generation, load demand, PHEV load, and grid energy price have most commonly been modeled using probabilistic approaches. Monte Carlo Simulation, cumulant-based method, probabilistic collection method, point estimate method, etc., are some widely used probabilistic approaches [61,62]. PEMs have been widely used since it provides a trade-off between accuracy and computation burden.

Hong's point estimate method (PEM) is used to evaluate statistical moments of a random quantity. The random quantity can be a function

Algorithm 1: STEP-2 - Finding PHEV charging energy requirement

$PHEV = zeros(nd,5)$; $fun1 = @P_{EV}^{MAX}(1-exp[\frac{-\alpha t}{tm2}])$;
$fun2 = @P_{EV}^{max}(\frac{tmax-t}{tmax-tm2})$;
for $jj = 1:1:nd$ **do**
  Find t in Eq. (31)) using Newton-Raphson algorithm (Use 2); $iter = 0$; $tl = t$; $t = tl$; $conv = 0$;
  if $tm2 - t > 0.01$ **then**
    while $conv == 0$ && $iter < 10$ **do**
      $iter = iter + 1$; $tu = tl + 1$; $time = 1$;
      if $tu > tm2$ **then**
        $thigh = 4.5$; $tm = tu - tl$;
      end
      $PEV(iter) = integral(fun1, tl, tu)$; $tl = tu$;
      if $tu == tm2$ **then**
        conv=1;
      end
    end
    $tn = 1 - tm$; $tl = tm2$; $tu1 = tm2 + tn$;
    $tu = min([tu1 \quad tmax])$;
    $PEV(iter) = PEV(iter) + integral(fun2, tl, tu)$; $tl = tu$;
    $tu = tmax$; $PEV(iter+1) = integral(fun2, tl, tu)$
  else
    $tl = t$; $tu = tmax$; $PEV(1) = integral(fun2, tl, tu)$;
  end
  $temp = size(PEV)$; $n = temp(1,2)$; $conv = 0$; $ii = 0$;
  while $conv == 0$ && $ii \le 6$ **do**
    $ii = ii + 1$; $PHEV(jj, ii) = PEV(ii)$;
    if $ii \ge 5$ || $ii \ge n$ **then**
      $conv = 1$
    end
  end
end
$tab1 = [PHEV \quad EV_E(:,2)]$;

Algorithm 2: Newton-Raphson method to estimate t in Eq. (31)

$EPEV = EV_E(jj, 1)$;
Initial guess of t;
if $EPEV \le E_{EV}(tm2)$ **then**
  $t = 0.01$
else
  $t = tm2 + 0.01$
end
Initialization: $tol = 1; \epsilon = 10^{-3}; iter = 0; itermax = 50;$
while $tol > \epsilon$ && $iter < itermax$ **do**
  $iter = iter + 1$;
  if $EPEV \le E_{EV}(tm2)$ **then**
    $J = P_{EV}^{MAX}(1-exp[\frac{-\alpha t}{tm2}])$; %Jacobian%
    $f = P_{EV}^{MAX}(t + (\frac{tm2}{\alpha})(exp[\frac{-\alpha t}{tm2}] - 1)) - EPEV$;
    %Function Value%
  else
    $J = P_{EV}^{MAX}(\frac{tmax-t}{tmax-tm2})$; %Jacobian%
    $f = (\frac{P_{EV}^{MAX}}{tmax-tm2})(tmax(t-tm2) - 0.5(t^2 - tm2^2)) - EPEV$;
    %Function Value%
  end
  $\Delta t = -\frac{-f}{J}$; $t = t + \Delta t$; $tol = |f|$;
end

Algorithm 3: STEP-4-PHEV charging load demands in different hours

```
cnt = 0;
for ii = 1 : 1 : 24 do
    if tab2(ii, 2) ≠ 0 then
        prob1 = tab2(ii, 2); t0 = ii;
        for kk = 1 : 1 : nd do
            prob2 = tab1(kk, tmax + 1);
            for jj = 1 : 1 : tmax do
                cnt = cnt + 1; t01 = t0 + jj − 1; if to1 > 24 then
                    t01 = t01 − 24;
                end
                tab3(cnt, 1) = t01; % Hour Number %
                tab3(cnt, 2) = tab1(kk, jj); % Energy demand %
                tab3(cnt, 3) = prob1 × prob2; % Probability %
            end
        end
    end
end
```

Algorithm 4: STEP 5- Filtering out PHEV states & probability for a hour *hr*

```
cnt = 0;  sumcheck = 0;
for ii = 1 : 1 : ndata do
    if tab3(ii, 1) == hr then
        cnt = cnt + 1;
        tab4(cnt, 1) = tab3(ii, 2); % Energy demand state of PHEV%
        tab4(cnt, 2) = tab3(ii, 3); % Probability%
        sumcheck = sumcheck + tab4(cnt, 2);
    end
end
tab4(cnt + 1, 1) = 0;% Zero charging energy demand state %
tab4(cnt + 1, 2) = 1 − sumcheck % Probability of zero charging energy demand %;
```

of one or multiple random stochastic input variables. The "Hong's 2 m PEM" applies to both symmetric and asymmetric variables [63]. Let **Z** denote a vector of the stochastic output variable. Further, the output is a function (**F**) of m uncertain input random variables. Let p_i denotes the ith random input variable.

$$\mathbf{Z} = \mathbf{F}(p_1, p_2, \ldots, p_i, \ldots, p_m) \tag{16}$$

"Hong's PEM" evaluates the probability concentrations at K locations for every input uncertain variable. The moments of the stochastic input variables are utilized to evaluate the concentrations. "2 m PEM" is used in this paper. In other words, two evaluations (at two locations) are carried out for each of the random input variables.

The kth concentration for the lth input random variable comprises a pair of location ($p_{l,k}$) and weight ($w_{l,k}$). The evaluation is carried out at the location, while the weight is a measure of the relative importance of the evaluation. The weights should add up to unity, i.e.,

$$\sum_{k=1}^{K}\sum_{l=1}^{m} w_{l,k} = 1 \tag{17}$$

$K = 2$ for "2 m PEM". The vector of outputs for the kth evaluation corresponding to the lth input random variable is evaluated by the following relation:

$$\mathbf{Z}(l,k) = \mathbf{F}(\mu_{p1}, \mu_{p2}, \ldots, p_{l,k}, \ldots, \mu_{pm}) \tag{18}$$

Algorithm 5: Overall algorithm

```
Start with Initial Incentive Value INC = 0;
while INC < 400 do
    Read Hong's 2 m PEM data for the hour;
    for t=1:1:24 do
        if Peak period then
            I(t) = INC;
        else
            I(t) = 0;
        end
        Compute modified load profile using Eq. (32), Eq. (33), Eq. (34);
    end
    Start Dynamic Programming (DP) for BESS;
    while DP does not converge do
        for t=1:1:24 do
            Carry out ELD using PSO and Hong's 2 m PEM (see algorithms 6);
            Compute Expected TOC and store;
        end
    end
    Increase INC ;
end
Find the daily minimum expected TOC;
```

Algorithm 6: Particle Swarm Optimization

```
Set iteration count IT = 0;
while IT ≤ ITMAX do
    WT = 0.9 + (0.4 − 0.9)(IT / ITMAX);
    for jj = 1 ... NPOP do
        for kk = 1 : 1 : NVARS do
            if IT == 0 then
                %Generate population randomly%
                pos(jj, kk) = pos⁻(kk) + rand(1) × (pos⁺(kk) − pos⁻(kk));
                vel(jj, kk) = 0
            else
                %Update particle positions and velocities%
                vel(jj, kk) = WT × vel(jj, kk) + 2.0 × rand(1) × (pbest(jj, kk) − pos(jj, kk)) + 2.0 × rand(1) × (gbest(kk) − pos(jj, kk));
                pos(jj, kk) = pos(jj, kk) + vel(jj, kk);
                if Limits are hit then
                    Set positions to maximum/minimum limits
                end
            end
        end
        Use algorithm 7 to perform Hong's PEM using control variables (pos(jj, kk)  ∀  kk = {1, 2, ..., NVARS});
        Evaluate the fitness function;
        Find local best (pbest);
    end
    Find global best (gbest);
    IT = IT + 1
end
```

where μ_{pi} denotes the mean of the ith input stochastic variable. The location and weight of the kth concentration for the lth input uncertain variable are evaluated using the following calculation steps:

Algorithm 7: Hong's $2m$ PEM method

Collect values of control variables from the PSO algorithm;
Obtain discrete probability distribution for each input uncertain variable from pdfs (see Section 2.1);
Find expectation (μ_{pi}) and standard deviation (σ_{pi}) from the discrete distribution for each input uncertain variable;
for $l = 1 \dots m$ **do**
  Calculate third central moment using Eq. (19);
  Calculate coefficient of skewness using Eq. (20);
  Calculate ζ_l using Eq. (21);
  for $k = 1 \dots 2$ **do**
    Calculate the standard location using Eq. (22);
    Calculate locations and weights using Eq. (23) ;
    Set input variables to $(\mu_{p1}, \mu_{p2}, \dots p_{l,k}, \dots, \mu_{pm})$ and use control variables from the PSO algorithm ;
    Carry out a deterministic power flow ;
    Compute output state variables from the power flow (i.e., solve Eq. (18));
  end
end
Compute the hourly expected value of the objective (use Eq. (24) with $j = 1$);

- Find the third central moment ($M_3(p_l)$)

$$M_3(p_l) = E[(p_l - \mu_{pl})^3] \quad l \in \{1, 2, \dots, m\} \tag{19}$$

$E[.]$ denotes expectation.

- Find the coefficient of skewness ($\lambda_{l,3}$)

$$\lambda_{l,3} = \frac{M_3(pl)}{\sigma_{pl}^3} \quad l \in \{1, 2, \dots, m\} \tag{20}$$

σ_{pl} is the standard deviation

- Calculate ς_l

$$\varsigma_l = 2\sqrt{m + (\frac{\lambda_{l,3}}{2})^2} \quad : l \in \{1, 2, \dots, m\} \tag{21}$$

- Calculate the standard location ($\xi_{l,k}$)

$$\xi_{l,k} = \frac{\lambda_{l,3}}{2} + (-1)^{3-k}\frac{\varsigma_l}{2} \quad : l \in \{1, 2, \dots, m\}, k \in \{1, 2\} \tag{22}$$

- Evaluate the location and weight.

$$\begin{cases} p_{l,k} = \mu_{pl} + \xi_{l,k}\sigma_{pl} & : l \in \{1, 2, \dots, m\}, k \in \{1, 2\} \\ w_{l,k} = \frac{(-1)^k}{m}\frac{\xi_{l,3-k}}{\varsigma_l} & : l \in \{1, 2, \dots, m\}, k \in \{1, 2\} \end{cases} \tag{23}$$

The jth moment of the output is evaluated using the following relation:

$$E(\mathbf{Z}^j) = \sum_{k=1}^{2}\sum_{l=1}^{m} w_{l,k}(\mathbf{Z}(l,k))^j \tag{24}$$

A few sample points and associated weights are computed from pdfs of uncertain input variables for a PEM method. Sample points and the corresponding weights are called concentrations. A deterministic study is carried out for each concentration individually. Raw/central /standard moments are computed for each of the output variables using the output of the deterministic study and the associated weight. The procedure for stochastic optimization incorporating the PEM is shown in algorithm 7. More on "Hong's PEM" can be found in [63–65].

Although Hong's PEM has been widely used for modeling power system uncertainties,most applications of Hong's PEM pertain to modeling renewable generation and load demand. On the other hand, the stochastic nature of the EV/PHEV charging load has most frequently been modeled using Monte Carlo Simulation (MCS) [28,29,31,33,38], and rarely using the Hong's PEM. Some other approaches like information gap decision theory (IGDT) [37,39], queuing model followed by a neural net [66], ARIMA model [5], wavelet transform [19], sequence operation theory [20], Markov Chain [22], Annealing PSO [25], sample average approximation method [36], etc., have also been reported. In contrast, the probabilistic nature of the PHEV charging demand has been modeled using Hong's PEM in this paper. A summary of the PHEV modeling method is provided in Table 2. Further, detailed algorithms for modeling hourly PHEV load states from the Hong's PEM data are provided in this paper. To the best of the author's knowledge, no similar algorithm for computing hourly PHEV charging requirements from Hong's PEM data has been discussed in detail so far in the literature.

Table 2
Modeling techniques for EV/PHEV charging load.

Sl.no	Ref.	EV load modeling techniques
1	[66]	Queuing model followed by a neural network
2	[5]	ARIMA model
3	[19]	Wavelet transform, particle swarm optimization and support vector machine
4	[20]	Sequence operation theory
5	[22]	Markov chain Monte Carlo
6	[25]	Annealing PSO
7	[27]	Not clearly mentioned
8	[28]	Monte carlo
9	[29]	Monte carlo
10	[31]	Monte carlo
11	[33]	Monte carlo
12	[36]	SAA (Sample Average Approximation) method
13	[37]	IGDT (information gap decision theory) method
14	[38]	Monte carlo
15	[39]	IGDT method

In this paper, a single wind farm at one location has been considered. Therefore, spatial correlations between wind speeds at different locations are not needed. Research has revealed a weak anti-correlation between solar irradiance and wind speed [67]. The correlation is considered while deriving the wind speed and solar irradiance pdf models for a given hour. Powers generated by SPGs and WPGs are fed to the stochastic power flow program. SPG and WPG are controlled independently. Therefore, power outputs of WPG and SPG (and also the load demand) are most commonly assumed to be uncorrelated for a power system analysis [38,43,58,68–70]. Similarly, researchers commonly assume pdfs of daily driven distance and charging pattern to be uncorrelated [27,31,33,38]. Recently, some researchers have focused on investigating correlated probability distributions [62]. Methods using different copula theories have been proposed. Alternatively, multivariate distribution models using the Morgenstern model, Nataf model, etc., have been proposed [71]. Nataf transformation followed by Hong's PEM have recently been used in power system applications [72,73]. Independent probability distributions have been considered in this paper in line with the approach given in [27,31,33,38,38,43,58,68–70]. However, the proposed method can be amended to incorporate correlations between different stochastic variables. Nataf transformation followed by Hong's PEM can be used in the proposed energy management approach [72,73]. The same shall be taken up in the future by the authors.

3. Smart transformer and PHEV load model

3.1. Smart transformer

An ST comprises a low-frequency transformer in conjunction with a power electronic converter system. An ST is equipped with advanced "control and communication" features. An ST can be deployed for providing ancillary services to the grid, addressing power quality (PQ)

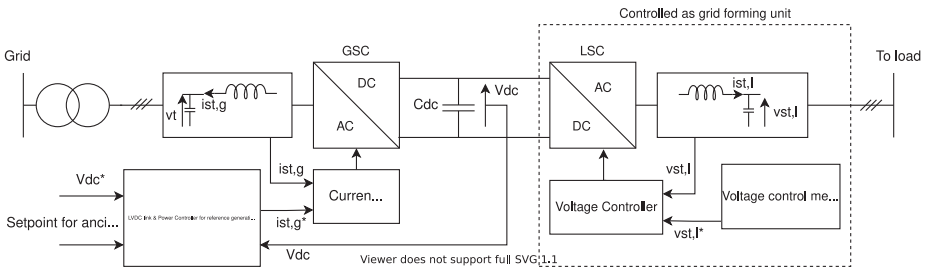

Fig. 1. Schematic of a smart transformer.

issues in the low/medium voltage distribution system, providing connectivity to DC loads through the DC link, etc. [47]. The schematic of an ST is shown in Fig. 1.

A two-stage back-to-back converter is considered in this paper. The AC/DC converter is present on the high voltage (HV) grid side and is named the grid side converter (GSC). The DC/AC converter is on the medium voltage (MV) load side and is called a load side converter (LSC). There is a DC link between the two converters. The DC link can also be used to feed DC loads present in the system. The two-stage back-to-back converter allows a decoupled control of the LSC and the GSC. The LSC is controlled as a grid forming inverter and produces a sinusoidal voltage of specified magnitude and frequency. On the other hand, the GSC is controlled to maintain the DC link voltage. One degree of freedom is available in the control scheme of the GSC, which may be used to provide ancillary services like voltage/reactive power support to the grid.

A voltage control algorithm can be integrated into the control of the LSC. The voltage control algorithm will provide the voltage set-point ($V^*_{STMV}(t)$) at every time step for the grid forming/LSC unit. Following performance indicators (PI) have been defined in the literature to assess the voltage dip or swell in a distribution network [74]:

(i) Voltage Rise Margin (VRM) [74]: The voltage rise margin (VRM) for concentration k at any hour t ($VRM_s(t)$)is calculated as follows:

$$VRM(l,k,t) = V^{GC}_{max} - \max\{V_i(l,k,t)\} \quad \forall i \in \Omega_B, \forall l \in \Omega_m, \forall k \in \Omega_k, \forall t \in \Omega_t \tag{25}$$

V^{GC}_{max} is the maximum allowed voltage in a network as per grid code requirement, $V_i(l,k,t)$ is the voltage magnitude at time t at the ith bus for the kth concentration. Ω_b, and Ω_t represent sets of buses and time respectively. $\Omega_k = \{1,2\}$, $\Omega_m = \{1,2,\ldots,m\}$. The expected VRM at any hour t ($E(VRM(t))$) is calculated as follows:

$$E(VRM(t)) = \sum_{k=1}^{2}\sum_{l=1}^{m} VRM(l,k,t) w_{l,k} \quad \forall t \in \Omega_t \tag{26}$$

A positive expected value of VRM indicates that there is no voltage swell in the network. V^{GC}_{max} is set to 1.05 pu in line with ANSI C84.1 requirement.

(ii) Voltage Drop Margin (VDM) [74]: VDM is a measure of the voltage dip in a distribution network. This PI has become more relevant with the introduction of the PHEV charging load, which is likely to cause a poor voltage profile in the network. The VDM for the concentration k at any hour t ($VDM(l,k,t)$) is calculated as follows:

$$VDM(l,k,t) = min(V_i(l,k,t) - V^{GC}_{min}) \quad \forall i \in \Omega_B \; l \in \Omega_m, \forall k \in \Omega_k, \forall t \in \Omega_t \tag{27}$$

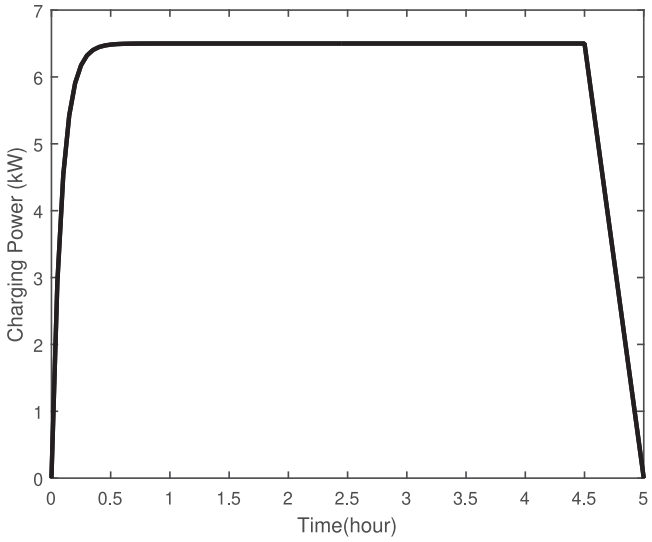

Fig. 2. PHEV battery charging characteristic.

The lowest allowed voltage as per grid code is denoted by V^{GC}_{min}. The expected VDM ($E(VDM(t))$) is computed as follows:

$$E(VDM(t)) = \sum_{k=1}^{2}\sum_{l=1}^{m} VDM(l,k,t) w_{l,k} \quad \forall t \in \Omega_t \tag{28}$$

A positive $E(VDM(t))$ indicates that there is no issue of voltage dip in the network. V^{GC}_{min} is set to 0.95 pu in sync with ANSI C84.1 requirement.

(iii) Average Voltage deviation (AVD): AVD for the concentration k at a time t is defined as follows:

$$AVD(l,k,t) = \frac{\sum_{i=1}^{NB}(|V_i(l,k,t) - 1.0|)}{NB} \tag{29}$$

NB is the number of system buses. The voltages are expressed in per unit in Eq. (29). The expected AVD ($E(AVD(t))$) is computed as follows:

$$E(AVD(t)) = \sum_{k=1}^{2}\sum_{l=1}^{m} AVD(l,k,t) w_{l,k} \quad \forall t \in \Omega_t \tag{30}$$

The objective of the voltage control scheme is to minimize $E(VDM(t))$. In other words, $V^*_{STMV}(t)$ is selected so as to minimize $E(VDM(t))$. Optimal $V^*_{STMV}(t)$ should also give positive $E(VDM(t))$ and $E(VRM(t))$ to comply with the grid power quality (PQ) requirements.

3.2. PHEV load model

The charging characteristic of a typical PHEV battery is shown in Fig. 2. The PHEV charging load at any time t ($P_{CHEV}(t)$) is modeled

using the following equations [75]:

$$P_{CHEV}(t) = \begin{cases} P_{EV}^{max}(1 - exp[\frac{-\alpha_{EV} t}{tm2}]) & : 0 < t \leq tm2 \\ P_{EV}^{max}(\frac{tmax - t}{tmax - tm2}) & : tm2 < t \leq tmax \\ 0 & : t > tmax \end{cases} \quad (31)$$

Following values are considered in this paper: $P_{EV}^{max} = 6.5$ kW, $\alpha_{EV} = 53.92$, $tm2 = 4.5$ h, $tmax = 5$ h [27,75]. The parameters pertain to a "Nissan Altra lithium-ion battery". The energy of the battery at $t = tm2$ is $E_{EV}(tm2) = 28.707$ kWh.

The algorithm for calculating the PHEV load demand is as follows:

- *STEP-1*: Calculate the daily distance traveled with the corresponding probability using the log-normal pdf of the daily traveled distance given in Eq. (9). The existing SOC and the energy (kWh) corresponding to each traveled distance are calculated using Eq. (11). The data is stored in a table named EV_E. The first column stores the remaining energy in kWh. The second column stores the corresponding probability. Let there be nd rows, corresponding to each driven distance.
- *STEP-2*: The maximum charging time is $tmax = 5$ hours. In this step, the charging energy requirement of the battery is computed for five hours from the commencement of the charging process. Algorithms 1, and 2 are used. The charging energy requirement is stored in a table $tab1$. The table $tab1$ has nd numbers of rows. Each row corresponds to a driven distance calculated in STEP-1. The table $tab1$ has six (6) columns. The first five columns store the energy requirement of the PHEV battery for five hours from the charging commencement time. If the PHEV battery is fully charged before $tmax = 5$ h, then the entry corresponding to the column is 0. The sixth column stores the probability calculated in STEP-1.
- *STEP-3* A table $tab2$ is prepared to store the probability of the charging commencement process. The data is prepared using the pdf of the charging strategy (Eqs. (12)–(14)). The table has twenty-four (24) rows. Each row corresponds to an hour. There are two columns. The first column stores the time (hour), and the second column stores the probability that the charging starts at the particular hour. For instance, $tab2(19, 1)$ will have an entry 19, while $tab2(19, 2)$ will store the probability of the charging process starting at hour 19.
- *STEP-4* Use algorithm −3 to find the PHEV charging load demand at different hours with the corresponding probability. The data is stored in a table $tab3$ having three columns. The first column will store the hour number. The second column stores the energy demand for the hour in kWh. The third column stores the corresponding probability. Let there be $ndata$ number of rows.
- *STEP-5* The PHEV energy demand states for a particular hour along with corresponding probabilities can be filtered out using algorithm 4. The data will be stored in a table $tab4$. This table can be fed to the "Hong's 2 m PEM" module for calculation at every hour. $tab4$ has two columns. The first column stores the PHEV energy demand, while the second column stores the probability.

4. Mathematical formulation and solution strategy

The mathematical model and the solution strategy are presented in this section.

4.1. Mathematical formulation

4.1.1. Economic model of responsive load due to DR

Loads can be broadly classified into three categories. Critical devices are needed at a given time. Shiftable loads can be used at any other preferred time. Washing machines, dishwashers, etc., are some examples of shiftable loads. Reducible loads can be turned off at a given time.

- *IBDR:* The economic model of load due to the implementation of the IBDR program is obtained using the concept of demand price elasticity. The model also considers the consumer benefits. Elasticity is the ratio of per unit change in demand at any hour to per unit change in tariff at an hour. The modified load participating in the IBDR program is given by [76–78]:

$$PL_i^{DR}(l,k,t) = \eta PL_i^0(l,k,t)\{1 + El(t,t)\frac{\rho(l,k,t) - \rho_0(l,k,t) + I(t)}{\rho_0(l,k,t)} + \sum_{h=1,h\neq t}^{24} El(t,h)\frac{\rho(l,k,h) - \rho_0(l,k,h) + I(h)}{\rho_0(l,k,h)}\}$$
$$\forall l \in \Omega_m, \forall k \in \Omega_k, \forall t \in \Omega_t \quad (32)$$

$PL_i^{DR}(l,k,t)$ is the load at bus i participating in the DR program, η is the percentage of load participating in the DR program. $PL_i^0(l,k,t)$ is the original demand at bus i, $\rho(t)$ is spot electricity price, $\rho_0(t)$ is the initial electricity price for hour t. $I(t)$ is the incentive offered per unit of load curtailed or shifted during time t for participating in an incentive-based DR program. $El(t,t)$ and $E(t,h)$ denote the self-elasticity and cross elasticity respectively. Self-elasticity is always negative, while cross elasticity is always positive. In this work, a real-time pricing scheme is not used. Therefore, the spot price and the initial price of electricity are the same in Eq. (32). The modified load with implementation of an IBDR program ($PL_i(l,k,t)$) is given below:

$$PL_i(l,k,t) = (1-\eta)PL_i^0(l,k,t) + PL_i^{DR}(l,k,t) \quad \forall l \in \Omega_m, \forall k \in \Omega_k, \forall t \in \Omega_t \quad (33)$$

The load change with implementation of IBDR ($\Delta PL_i(l,k,t)$) is given by:

$$\Delta PL_i(l,k,t) = \eta PL_i^0(l,k,t) - PL_i^{DR}(l,k,t)\Delta \quad \forall l \in \Omega_m, \forall k \in \Omega_k, \forall t \in \Omega_t \quad (34)$$

- *PBDR:* Researchers have also proposed PBDR programs for microgrids. The electricity price and the usage demand in a PBDR program are related as follows [79,80]:

$$PL(t) = A(\rho_c(t))^{\epsilon} \quad (35)$$

The price rate is the ratio of the actual electricity price to the original electricity price for the customers in the MG. A twenty-one step price-elastic demand curve (price rate varying from 50% to 150% in steps of 5%) is used in this paper [80]. The value of ϵ is taken as (−0.2122) [79]. The PBDR model ($\forall i \in \Omega_b$, $\forall l \in \Omega_m$, $\forall k \in \{1,2\}$, $\forall t \in \Omega_t$) is as follows [79,80]:

$$\begin{cases} PL_i(l,k,t) = E(PL_i^0(t))\sum_j \nu_j(t) r_j^{PBDR,P}(1 + LDU_i(l,k,t)) \\ \sum_j \nu_j(t) = 1; \quad \nu_j(t) \in \{0,1\} \end{cases} \quad (36)$$

$LDU_i(l,k,t)$ denotes the uncertainty in the predicted load demand. The value of $LDU_i(l,k,t)$ is taken from the Hong's 2 m PEM. When $LDU_i(l,k,t)$ is involved, uncertainty of the PBDR scheme is fully considered [79,80].

4.1.2. Master-problem

The problem is solved using a bi-level approach. The expected average voltage deviation is minimized at each hour. It is mathematically stated as follows:

$$\underset{V_{STMV}^*(t)\in[0.95,1.05]}{\text{minimize}} \; E(AVD(V_{STMV}^*(t))) \quad \forall t \in \Omega_t \quad (37)$$

subject to:

$$E(VRM(t)) > 0 \quad \forall t \in \Omega_t \quad (38)$$

$$E(VDM(t)) > 0 \quad \forall t \in \Omega_t \tag{39}$$

$$\mathbf{F}(\mathbf{V}^*_{\mathbf{STMV}}(\mathbf{t}), \mathbf{g_{l,k,t}}) = \mathbf{0} \quad \forall l \in \Omega_l, \forall k \in \Omega_k, \forall t \in \Omega_t \tag{40}$$

$$\mathbf{g_{l,k,t}} \in [\mathbf{gl}, \mathbf{gu}] \quad \forall l \in \Omega_l, \forall k \in \Omega_k, \forall t \in \Omega_t \tag{41}$$

Eq. (37) represents that the objective is to minimize the expected AVD at every time step (1 h in this paper). $V^*_{STMV}(t)$ is the control variable, which lies between the limits 0.95 pu and 1.05 pu. A step size of 1%, i.e., 0.01 pu is selected for the control variable [74]. Eqs. (38) and (38) ensure that there is no voltage swell or dip in the network. In other words, all the node voltages lie within the range [0.95, 1.05] pu in compliance with the ANSI C84.1 requirement. Eq. (40) stands for the power flow equations. $\mathbf{g_{l,k,t}}$ stands for the set of power system state variables (voltage magnitudes, phase angles, line currents). Eq. (41) ensures that all power system state variables are within acceptable limits [**gl**, **gu**].

4.1.3. Slave problem

The objective is to minimize the expected operating cost.

$$\underset{\mathbf{x(t)}\in\Omega_x}{\text{minimize}} \sum_{t\in\Omega_t} E(TOC(t)) \tag{42}$$

where $\mathbf{x(t)}$ stands for the control variables, Ω_x is the set of control variables, and $TOC(.)$ is the total operating cost.

$$\Omega_x = \{PG_i(t), PB(t), I(t)\} \quad \forall i \in \Omega_G, \forall t \in \Omega_t \tag{43}$$

where, $PG_i(t)$ denotes the active power injection of the ith dispatchable unit at time t, $PB(t)$ is the battery charging power, and $I(t)$ is the incentive value. Ω_G is the set of all dispatchable units, and Ω_t is the set of all times in a day. The total operating cost TOC is calculated as follows for the IBDR program:

$$\begin{aligned} TOC(l,k,t) =& P_{grid}(l,k,t)\rho(l,k,t) + \sum_{j\in\Omega_G} a_j + b_j PG_j(l,k,t) \\ &+ c_j(PG_j(l,k,t))^2 \\ &+ I(t)\sum_{i\in\Omega_B} \Delta PL_i(l,k,t) \quad \forall l \in \Omega_l, \forall k \in \Omega_k, \forall t \in \Omega_t \end{aligned} \tag{44}$$

$P_{grid}(.)$ denotes the power imported from the sub-station/main-grid, Ω_B is the set of system buses. a_i, b_i, and c_i are fuel cost coefficients of dispatchable unit i. The first term in Eq. (44) denotes the cost of energy purchase from the grid. The second term represents the fuel cost of dispatchable generators. The third term stands for the expense of paying incentives to the customers participating in the DR program. In Eq. (44), $P_{grid}(.) > 0$, when power is imported from the main-grid. When power is sold to the main grid, $P_{grid}(.) < 0$.

The TOC for the PBDR program will comprise the energy cost of the grid power and fuel costs of dispatchable units minus earnings by selling power to customers:

$$\begin{aligned} TOC(l,k,t) =& P_{grid}(l,k,t)\rho(l,k,t) + \sum_{j\in\Omega_G} a_j + b_j PG_j(l,k,t) \\ &+ c_j(PG_j(l,k,t))^2 \\ &- \sum_{i\in\Omega_B} E(PL_i^0(t)) \sum_{j\in\Omega_J} \nu_j(t) r_j^{PBDR,P}(1 + LDU_i(l,k,t))\rho_{cj}(t) \\ &\forall l \in \Omega_l, \forall k \in \Omega_k, \forall t \in \Omega_t \end{aligned} \tag{45}$$

The third term in Eq. (45) denotes earnings by selling power to customers.

The operation is subject to several constraints as given below:

- *Power balance constraint:* The active and reactive power constraints at bus i are as follows:

$$\begin{aligned} &PG_i(l,k,t) + PW_i(l,k,t) + PS_i(l,k,t) + \Lambda_i P_{grid}(l,k,t) - PL_i(l,k,t) \\ &- P_{CHEVi}(l,k,t) - PB_i(l,k,t) = f1_i(l,k,t) \quad \forall l \in \Omega_m, \forall k \in \Omega_K, \forall t \in \Omega_t \end{aligned} \tag{46}$$

$$f1_i(l,k,t) = |V_i(l,k,t)| \sum_{j\in\Omega_B} |V_j(l,k,t)||Y_{ij}|cos(\delta_i(l,k,t) - \delta_j(l,k,t) - \theta_{ij}) \tag{47}$$

$$\begin{aligned} &QG_i(l,k,t) + QW_i(l,k,t) + QS_i(l,k,t) + \Lambda_i Q_{grid}(l,k,t) - QL_i(l,k,t) \\ &- Q_{CHEVi}(l,k,t) - QB_i(l,k,t) = f2_i(l,k,t) \quad \forall l \in \Omega_m, \forall k \in \Omega_K, \forall t \in \Omega_t \end{aligned} \tag{48}$$

$$f2_i(l,k,t) = |V_i(l,k,t)| \sum_{j\in\Omega_B} |V_j(l,k,t)||Y_{ij}|sin(\delta_i(l,k,t) - \delta_j(l,k,t) - \theta_{ij}) \tag{49}$$

  $\Lambda_i = 1$ if bus i is the slack-bus. Otherwise $\Lambda_i = 0$. $V_i(.)$ and $\delta_i(.)$ denote the voltage magnitude and angle at bus i. $|Y_{ij}|$ and θ_{ij} stand for the magnitude and angle of the ijth element of the Y-bus. $QG_i(.)$, $QW_i(.)$, $QS_i(.)$, $Q_{grid}(.)$ are the reactive power injections from the dispatchable unit, WPG, SPG, and grid respectively. $QL_i(.)$, $QB_i(.)$, $Q_{CHEVi}(.)$ are the reactive power load, reactive power fed to the battery converter, and EV charger respectively. The suffix i denotes that the particular unit is connected to bus i. Eqs. (46) and (48) represent the active and reactive power balance at bus i.
- *Unit capacity constraint:* The ratings of the units cannot be exceeded:

$$\begin{cases} PG_i^{min} \le PG_i(l,k,t) \le PG_i^{max} & : \forall i \in \Omega_G, \forall l \in \Omega_m, \\ \quad \forall k \in \Omega_k, \forall t \in \Omega_t \\ QG_i^{min} \le QG_i(l,k,t) \le QG_i^{max} & : \forall i \in \Omega_G, \forall l \in \Omega_m, \\ \quad \forall k \in \Omega_k, \forall t \in \Omega_t \end{cases} \tag{50}$$

  $PG_i^{min/max}$ and $QG_i^{min/max}$ denote the minimum/maximum active and reactive power handling capacity of unit i.
- *Line current constraint:* The line currents should be within acceptable limits:

$$|I_{ln}(l,k,t)| \le I_{ln}^{max} \quad : \forall ln \in \Omega_{ln}, \forall l \in \Omega_m, \forall k \in \Omega_k, \forall t \in \Omega_t \tag{51}$$

  Ω_{ln} is the set of all lines in the system. I_{ln}^{max} is the maximum line rating, while $I_{ln}(.)$ is the line current.
- *Battery storage constraint:* The battery energy storage system (BESS) should satisfy the following constraint ($\forall l \in \Omega_m$, $\forall k \in \Omega_k$, $\forall t \in \Omega_t$):

$$EBAT(l,k,t) = EBAT(l,k,t-1) + PB(l,k,t)\frac{\Delta T}{\eta_{dis}} \quad : PB(l,k,t) \le 0 \tag{52}$$

$$EBAT(l,k,t) = EBAT(l,k,t-1) + PB(l,k,t)\Delta T\eta_{chg} \quad : PB(l,k,t) > 0 \tag{53}$$

$$EBAT^{min} \le EBAT(l,k,t) \le EBAT^{max} \tag{54}$$

$$EBAT(l,k,0) = EBAT(l,k,T) \tag{55}$$

$$|PBAT(l,k,t)| \le PBAT^{rated} \tag{56}$$

Eqs. (52) and (53) are the battery discharging and charging equations. The battery energy must not exceed the maximum limit and should not fall below a specified threshold (Eq. (54)). The energy stored in the battery should be the same at the beginning and the end of the optimization horizon (Eq. (55)). The battery charging/discharging power should not exceed the rated values (Eq. (56)). $EBAT(.)$ denotes the energy of the battery. $\eta_{chg/dis}$ denotes the charging/discharging efficiency. $EBAT^{min/max}$ is the minimum/maximum battery energy specification. The rated battery power is $PBAT^{rated}$.

- *Power exchange constraint:* The converters and the ST have rated power handling capacities, which cannot be exceeded ($\forall l \in \Omega_m$, $\forall k \in \Omega_k$, $\forall t \in \Omega_t$).

$$\begin{cases} |P_{grid}(l,k,t)| \le P_{grid}^{max} \\ |Q_{grid}(l,k,t)| \le Q_{grid}^{max} \end{cases} \tag{57}$$

$P_{grid}^{max}/Q_{grid}^{max}$ is the maximum active/reactive power handling capacity of the LSC converter of the ST.

- *Constraints for PBDR:* Following two additional constraints should be satisfied for PBDR [79,80]:

$$\sum_{t\in\Omega_t}\sum_{i\in\Omega_B} E(PL_i^0(t)) \sum_{j\in\Omega_J} v_j(t) r_j^{PBDR,P} \rho_{cj}(t) \le \sum_{t-\in\Omega_t}\sum_{i\in\Omega_B} E(PL_i^0(t))\rho_{0c}(t) \tag{58}$$

$$\sum_{t\in\Omega_t}\sum_{i\in\Omega_B} E(PL_i^0(t)) \sum_{j\in\Omega_J} v_j(t) r_j^{PBDR,P} \ge \sum_{t-\in\Omega_t}\sum_{i\in\Omega_B} E(PL_i^0(t)) \tag{59}$$

Eq. (58) ensures that the customer bill does not increase after implementation of the PBDR. Eq. (59) guarantees that a customer does not need to reduce the daily consumption.

4.2. Solution strategy

The optimization problem is solved using a nested approach. Techniques used to solve different optimization problems are as follows:

4.2.1. Master problem

The master problem is to find the optimal setpoints for the LSC of the ST for minimizing the average voltage deviation. Further, all the bus voltages must comply with ANSI C84.1 requirements. The optimization problem is solved as a day ahead optimization problem with hourly stochastic forecasts. Therefore, an exhaustive search method is used. The limits for setpoint are 1.05 pu and 0.95 pu. A step size of 1%, i.e., 0.01 pu is used [74].

4.2.2. Slave problem

The objective is to find optimal incentive values, schedule for dispatchable generators, and BESS to minimize the TOC. Following techniques have been adopted:

- The incentive value is optimized using an exhaustive search method. Alternatively, heuristic approaches like particle swarm optimization (PSO) may be used. PSO has been explained in detail in the literature [81] and is not repeated here for brevity.
- The hourly BESS scheduling is carried out using discrete dynamic programming. More on discrete dynamic programming can be found in [82].
- The dispatchable units are scheduled optimally using PSO. More on scheduling dispatchable units using PSO is available in [83]. The active power outputs from dispatchable units are taken as control variables. Active and reactive power equality constraints are satisfied by running a forward–backward distribution power flow. The active and reactive power supplied/consumed by the LSC of ST act as slack variables.

The power flow problem is solved using the backward–forward distribution load flow for radial distribution level networks. All DG units are modeled as negative loads. Buses to which DG units are connected are modeled as PQ buses. The power injected by a renewable source is obtained from the solar irradiation (SPG) and wind speed (WPG) data. Power injections of dispatchable units come from the ELD program. The BESS is also modeled as a constant power source for a particular hour. The BESS acts as a load during the charging process. The BESS is modeled as a negative load during the discharging process. The LSC of the ST is considered as the slack bus. The active and reactive power supplied by the LSC act as slack variables. The voltage of the slack bus is determined using the proposed voltage control strategy. More on distribution power flow can be found in [84]. PSO is implemented as follows:

- *Control variables:* Active power generations of dispatchable units are taken as control variables.
- *Satisfaction of Equality constraints:* Active and reactive power balances in the system are satisfied by running a power flow program. Dispatchable and non-dispatchable units are modeled as negative loads in the power flow program. The power generation of a dispatchable source is fed from the PSO to the power flow program. Solution of the power flow gives the active and reactive power drawn from the LSC of the ST.
- *Limit handling:* If a control variable tries to violate the upper or the lower limit at any iteration step, the control variable is set to the boundary value being violated.
- *Satisfaction of inequality constraints:* Inequality constraints are handled using a penalty function approach.

Following parameters were used in the PSO program: trust parameters $c_1 = c_2 = 2.0$, maximum iterations = 60, population size = 40, initial weight = 0.90, final weight = 0.40. The flowchart for implementing the PSO algorithm is shown in algorithm 6. The nested optimization problem is solved using the flowchart shown in Fig. 3. The dynamic programming (DP) and ELD problems are solved within the IBDRP loop with modified load profiles. The optimal incentive value gives the minimum daily expected cost. Algorithm steps are shown in algorithm 5 and stated below:

- Step-1: The incentive value of the IBDRP is set in the outer loop.
- Step-2: The load profile is modified using the incentive value.
- Step-3: A dynamic programming (DP) is initiated considering the modified load profile for optimal BESS scheduling.
- Step-4: The ELD problem is solved within the DP loop with the modified load profile. The expected TOC is computed for every hour. Continue till the DP converges.
- Step-5: Increase the TOC value and go to Step-1. Continue till the maximum incentive value is reached.

The optimal incentive value gives the minimum daily expected cost.

5. Simulation study

5.1. Test system and input data

The proposed methodology is implemented on a thirty-three (33) bus radial distribution network. Peak active and reactive power demands are 3715 kW and 2300 kVAR, respectively. The substation voltage is 12.66 kV [85]. The distribution network is converted to a microgrid by integrating DG. The microgrid has two dispatchable units. A 2 MW Natural Gas Turbine (NGT) is located at bus #2. A 1 MW Biomass unit is located at bus #12. A BESS is present at bus 26. The battery parameters are adopted from [78]. A WPG of 0.5 MW is present at bus 18. Further, an SPG of 1 MW is present at bus 26. Sizes and locations of DG units are adopted from [78]. Further, all DG units (dispatchable and non-dispatchable) operate at the unity power factor.

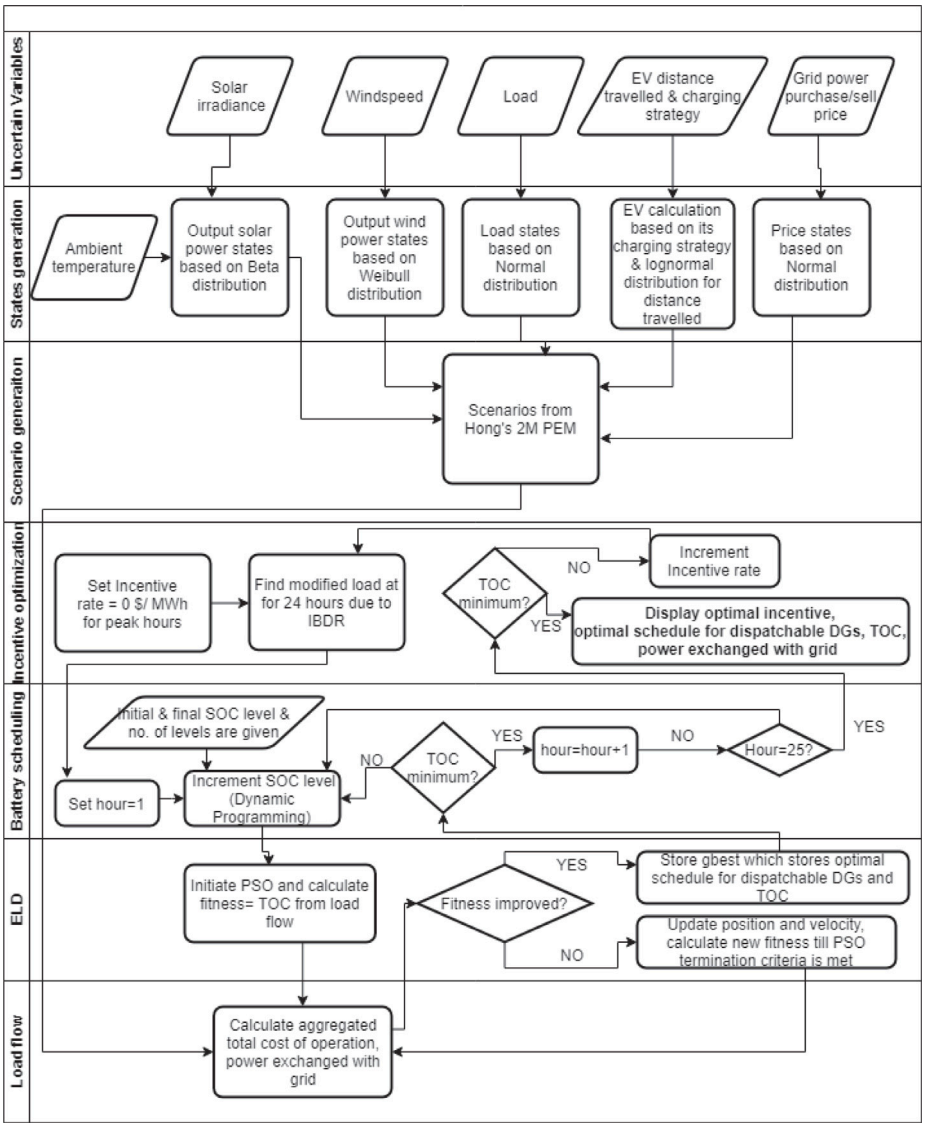

Fig. 3. Flowchart for solving the slave problem.

In other words, the dispatchable units inject only active power to the microgrid. The test system is shown in Fig. 4.

Historical data for solar irradiance and wind speed data are taken from [86]. The yearly data is divided into four seasons. May to July constitute the summer season. Autumn is from August to October. Winter ranges from November to January, while February to April is the spring season [87]. The annual data is divided into four seasons by averaging it over three months for each season for twenty-four hours. Temperature data for the region is obtained from [87]. Load profile data is taken from [88]. The load profile is divided into three categories. If the load demand is greater than 90% of the peak load, then it is the peak period. Similarly, if the load demand is lesser than equal to 70% of the peak demand , then it is the valley period. All periods with load demands ranging between 90% and 70% are considered off-peak periods. The grid energy price (mean) is 40 $/kWh during valley periods, 160 $/kWh during the off-peak periods , and 400 $/kWh during peak periods [78]. Further, it is assumed that all system buses (except the sub-station bus) cater to the charging requirement of three (03) PHEVs. Li-Ion batteries are considered for PHEVs. The peak charging power is 6.5 kW. The battery charging characteristic is shown in Fig. 2. The PHEV charging requirement imposes an additional load of 16.8% of the peak demand.

Table 3
Scenarios for IBDR.

Scenario name	Charging strategy	ELD	BESS	IBDR	ST
S1	Uncoordinated	Y	N	N	N
S2	Coordinated	Y	N	N	N
S3	Smart	Y	N	N	N
S4	Uncoordinated	Y	N	Y	N
S5	Coordinated	Y	N	Y	N
S6	Smart	Y	N	Y	N
S7	Uncoordinated	Y	Y	Y	N
S8	Coordinated	Y	Y	Y	N
S9	Smart	Y	Y	Y	N
S10	Uncoordinated	Y	Y	Y	Y
S11	Coordinated	Y	Y	Y	Y
S12	Smart	Y	Y	Y	Y

5.2. Simulation results

Simulation studies have been carried out by writing codes in MATLAB 2020*b* on an Intel core *i*5, 2.7 GHz laptop with 8 GB RAM. It is assumed that 40% of the total load participates in the DR program. The load demand follows a "normal distribution" with a standard deviation

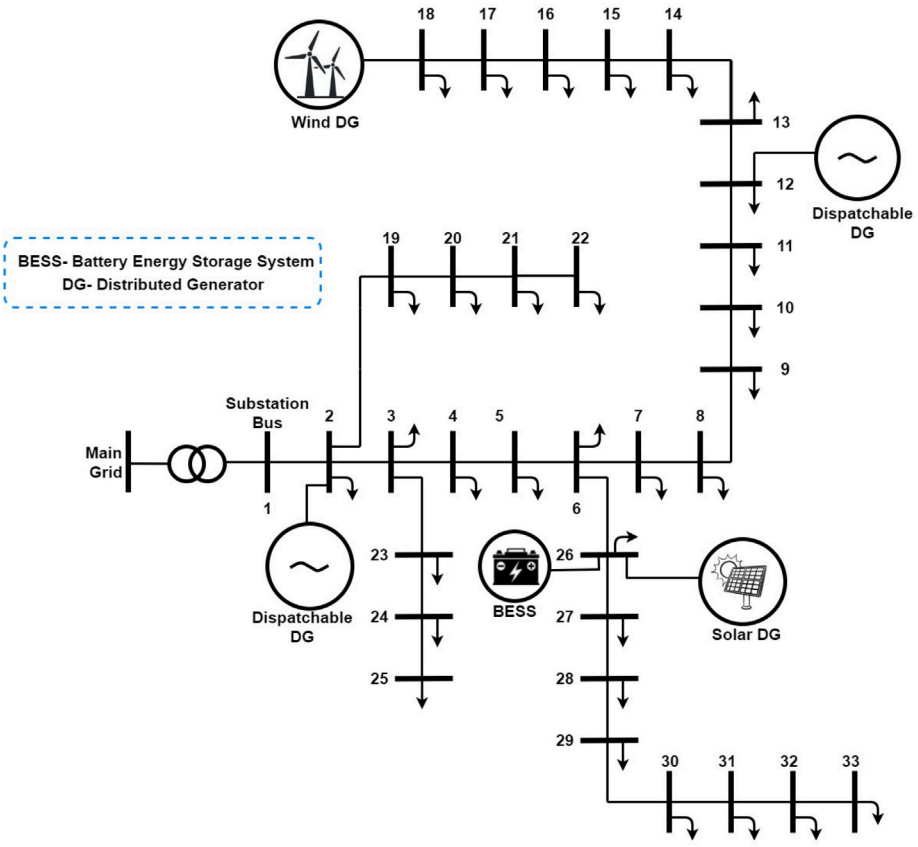

Fig. 4. Test system.

of 5% [89]. The grid energy price is also normally distributed with a standard deviation of 1%. Three different PHEV charging strategies have been considered in this work. Several scenarios, detailed below, have been considered. Details of scenarios are given in Table 3.

5.2.1. Effect of charging strategies — scenarios S1, S2, S3

The uncoordinated charging strategy of EV is considered in scenario S1. The coordinated and uncoordinated strategies are considered in scenarios S2 and S3, respectively. Generations from dispatchable units are optimized in scenarios S1, S2, and S3. BESS and IBDR are not considered. The optimized results (expected cost and expected loss) for the three scenarios are shown in Table 3. The expected TOC for scenarios S1, S2, and S3 are $15 851.73, $15 757.48, and $15 627.23 respectively. The expected TOC is the maximum for the uncoordinated charging strategy (S1) and the minimum for the smart charging strategy (S3). The TOC value lies in-between for the coordinated charging strategy (S2). The expected TOC is reduced by ∼0.59% using a coordinated charging strategy. The smart charging strategy reduces the expected TOC by ∼1.41%. The expected loss for uncoordinated (S1), coordinated (s2), and smart (S3) charging strategies are 2076.73 kWh, 2082.69 kWh, and 2076.89 kWh respectively. Therefore, the loss is the minimum for the uncoordinated charging strategy (S1) and only slightly higher for the smart charging strategy (S3). The loss is ∼0.29% higher with the coordinated charging strategy (S2) (see Table 4).

Expected generations in different scenarios are shown in Fig. 5 The grid power price is low during the daytime. Hence, the bulk of the power requirement is met from the grid during the daytime. The dispatchable units (NGT and biomass) generate minimum power. On the other hand, the grid power price is high in the evening (peak period). Hence, the dispatchable units (NGT and biomass) increase their outputs while the grid power reduces. The trend is common for scenarios S1 (Fig. 5a), S2 (Fig. 5b), and S3 (Fig. 5c).

5.3. Implementation of IBDR

IBDR is implemented for three different charging strategies. The incentive offered to the participating customers is optimized. The dispatchable units are also scheduled to minimize the operating cost. The expected TOC is minimum for an incentive value of 203 $/MWh for the uncoordinated charging strategy (see Fig. 6a). Therefore, the optimal incentive value for uncoordinated charging is 203 $/MWh. The optimal incentive values for coordinated charging and smart charging are 207 $/MWh and 203 $/MWh respectively (see Figs. 6b and 6c respectively). The expected effective load profiles with different PHEV charging strategies and IBDR are shown in Fig. 7.

Expected losses and TOC are tabulated in Table 5 for the three charging strategies (Scenarios S4, S5, and S6). The expected daily TOCs are $13 285.93, $13 178.81, and $13 067.38, respectively, for scenarios S4, S5, and S6. The expected losses are 1500.58 kWh, 1481.43 kWh, and 1516.27 kWh for scenarios S4, S5, and S6, respectively. The expected TOC in scenario S4 (uncoordinated charging) is lower by ∼16.19% than scenario S1. The expected loss reduces by ∼27.74%. For the coordinated charging strategy, the IBDR with optimized incentive value reduces the expected TOC by ∼16.36% and the expected loss by ∼28.87% (comparison of scenarios S4 and S1). In the case of a smart charging strategy, the reduction in expected losses and expected TOC are ∼16.38% and ∼26.99% respectively (comparison of scenarios S3 and S6). Therefore, an optimal IBDR program reduces the expected TOC and loss significantly.

The expected generation from dispatchable units and the power exchanged with the grid are shown in Figs. 5d, 5e, and 5f for scenarios S4, S5, and S6 respectively. The grid meets the bulk of the power requirement during off-peak and valley periods, Power generations from dispatchable sources are low during off-peak and valley periods. The grid energy price is high during the peak period. Therefore,

Table 4
Impact of charging strategies — expected loss and TOC.

Hour	S1		S2		S3	
	Loss (kWh)	TOC ($/h)	Loss (kWh)	TOC ($/h)	Loss (kWh)	TOC ($/h)
1	57.27	135.62	58.03	136.48	61.28	139.91
2	50.59	131.15	50.73	131.31	54.42	135.39
3	47.26	128.64	47.28	128.65	50.57	132.4
4	43.95	126.04	43.94	126.01	46.51	129.05
5	43.14	125.09	43.14	125.09	44.98	127.26
6	44.79	125.36	44.79	125.36	45.99	126.77
7	51.98	129.12	51.98	129.12	52.71	129.95
8	66.19	384.49	66.19	384.49	66.56	386.25
9	87.93	436.21	87.93	436.21	88.14	437.06
10	93.15	806.76	93.15	806.76	93.19	807.66
11	101.03	836.97	101.03	836.97	101.05	837.33
12	103.44	854.29	103.44	854.29	103.39	853.92
13	101.4	919.56	101.4	919.56	101.38	919.44
14	105.84	965.87	105.84	965.87	105.82	965.7
15	108.65	1003.88	108.65	1003.88	108.6	1003.38
16	105.02	1007.46	105.02	1007.46	105.05	1007.84
17	107.13	1050.68	107.13	1050.68	107.22	1051.67
18	134.42	1328.79	111.85	1103.61	112.08	1105.93
19	112.8	1150.81	104.99	1068.79	105.47	1073.66
20	104.62	1077.29	102.69	1056.28	103.58	1065.44
21	103.12	1060.96	110.09	1131.98	104.23	1072.21
22	105.46	1073.94	115.6	1176.17	107.74	1096.98
23	119.64	543.99	135.83	589.27	124.45	557.53
24	77.91	448.75	81.98	463.18	82.48	464.52
Total	**2076.73**	**15851.73**	**2082.69**	**15757.48**	**2076.89**	**15627.23**

Table 5
Impact of IBDR for different charging strategies.

Hour	S4		S5		S6	
	Loss (kWh)	TOC ($/h)	Loss (kWh)	TOC ($/h)	Loss (kWh)	TOC ($/h)
1	61.5	138.8	63.1	140.24	65.69	143.1
2	54.34	134.13	55.18	134.83	58.32	138.37
3	50.76	131.51	51.43	132.05	54.2	135.27
4	47.2	128.81	47.8	129.28	49.87	131.82
5	46.38	127.86	46.98	128.37	48.3	130.03
6	48.2	128.23	48.84	128.75	49.45	129.64
7	56.02	132.29	56.78	132.87	56.78	133.12
8	73.21	404.71	64.8	380.34	73.61	406.47
9	97.4	459.58	86.05	431.41	97.79	460.43
10	56.16	608.49	56.45	614.42	56.18	609.37
11	60.79	629.67	61.1	635.86	60.79	630.02
12	61.88	644.53	62.2	650.79	61.85	644.26
13	55.3	709.92	55.67	716.14	55.29	709.82
14	56.78	753.11	57.18	759.4	56.77	752.98
15	57.66	790.35	58.09	796.65	57.63	789.95
16	55.71	800.39	56.15	806.51	55.72	800.76
17	55.96	844.8	56.4	850.86	56	845.77
18	68.66	1117.1	58.06	902.56	57.73	898.76
19	57.99	949.27	54.67	874.75	54.46	873.64
20	54.03	879.37	53.56	864.58	53.57	867.75
21	53.31	863.35	57.3	938.81	53.88	874.38
22	54.3	873.85	59.89	979.96	55.45	896.44
23	131.46	567.74	133.35	590.18	136.53	581.34
24	85.58	468.07	80.4	459.2	90.41	483.89
Total	**1500.58**	**13285.93**	**1481.43**	**13178.81**	**1516.27**	**13067.38**

Table 6
Impact of BESS scheduling for different charging strategies.

Hour	S7		S8		S9	
	Loss (kWh)	TOC ($/h)	Loss (kWh)	TOC ($/h)	Loss (kWh)	TOC ($/h)
1	63.7	141.14	65.34	142.58	68.03	145.44
2	54.34	134.13	55.18	134.83	58.32	138.37
3	50.76	131.51	51.43	132.05	54.2	135.27
4	51.19	133.46	51.81	133.81	54.05	136.48
5	50.27	132.51	50.91	133.01	52.33	134.68
6	52.03	132.87	52.7	133.4	53.37	134.29
7	59.92	136.94	60.72	137.52	60.74	137.77
8	73.21	404.71	64.8	380.34	73.61	406.47
9	97.4	459.58	86.06	431.41	97.62	460.43
10	56.16	608.49	56.45	614.42	56.16	609.37
11	60.79	629.67	61.1	635.86	60.79	630.02
12	61.88	644.53	62.2	650.79	61.85	642.83
13	55.3	709.92	55.67	716.14	55.29	709.26
14	56.78	753.11	57.18	759.4	56.77	752.19
15	57.66	790.35	58.09	796.65	57.63	787.3
16	55.71	800.39	56.13	806.51	55.72	800.76
17	55.96	844.8	56.4	850.86	56	845.77
18	60.11	992.1	56.07	861.24	54.07	857.44
19	53.68	866.48	52.76	833.45	52.55	832.34
20	52.08	838.05	53.56	864.58	51.67	826.46
21	53.31	863.35	53.07	856.05	51.95	833.07
22	54.3	873.85	55.23	897.04	53.4	813.87
23	131.46	567.74	133.3	590.18	136.53	581.34
24	94.07	496.37	88.68	487.47	99.79	512.25
Total	1512.07	13 086.05	1494.84	12 979.59	1532.44	12 863.47

Table 7
Impact of ST on expected loss and TOC.

Hour	S10			S11			S12		
	Setpt	Loss (kWh)	TOC ($/h)	Setpt	Loss (kWh)	TOC ($/h)	Setpt	Loss (kWh)	TOC ($/h)
1	1.03	59.77	140.98	1.03	61.31	142.42	1.03	63.82	145.27
2	1.02	52.08	134.04	1.02	52.88	134.74	1.02	55.89	138.27
3	1.02	48.65	131.42	1.02	49.29	131.96	1.02	51.95	135.18
4	1.02	49.07	133.37	1.02	49.66	133.88	1.02	51.8	136.39
5	1.02	48.19	132.42	1.02	48.8	132.93	1.02	50.16	134.6
6	1.02	49.87	132.79	1.02	50.51	133.31	1.02	51.15	134.2
7	1.03	56.23	136.79	1.03	56.98	137.37	1.03	56.99	137.62
8	1.03	68.67	403.98	1.02	62.09	379.91	1.03	69.04	405.74
9	1.03	91.28	458.6	1.03	80.68	430.55	1.03	91.49	459.45
10	1.01	55.02	608.03	1.01	55.3	613.96	1.01	55.02	608.91
11	1.01	59.55	629.17	1.01	59.85	635.36	1.01	59.55	629.52
12	1.01	60.61	644.03	1.01	60.93	650.28	1.01	60.59	643.75
13	1.01	54.16	709.46	1.01	54.52	715.68	1.01	54.15	709.36
14	1.01	55.6	752.63	1.01	56	758.92	1.01	55.59	752.5
15	1.01	56.46	789.87	1.01	56.88	796.17	1.01	56.43	789.47
16	1.01	54.55	799.93	1.01	54.96	806.04	1.01	54.56	800.3
17	1.02	53.66	843.88	1.02	54.08	849.93	1.02	53.7	844.85
18	1.02	57.62	991.1	1.02	53.76	860.31	1.01	52.94	815.79
19	1.02	51.47	865.59	1.02	50.59	832.58	1.02	50.39	831.48
20	1.02	49.93	837.19	1.02	51.35	863.7	1.02	49.55	825.61
21	1.02	51.12	862.47	1.02	50.88	855.18	1.02	49.81	832.22
22	1.02	52.06	872.96	1.02	52.95	896.12	1.02	51.21	854.21
23	1.04	120.44	565.98	1.04	122.11	588.39	1.04	125.06	579.5
24	1.03	88.16	495.43	1.03	83.12	486.59	1.03	93.51	511.26
Total		**1444.22**	**13 072.11**		**1429.48**	**12 966.28**		**1464.35**	**12 855.45**

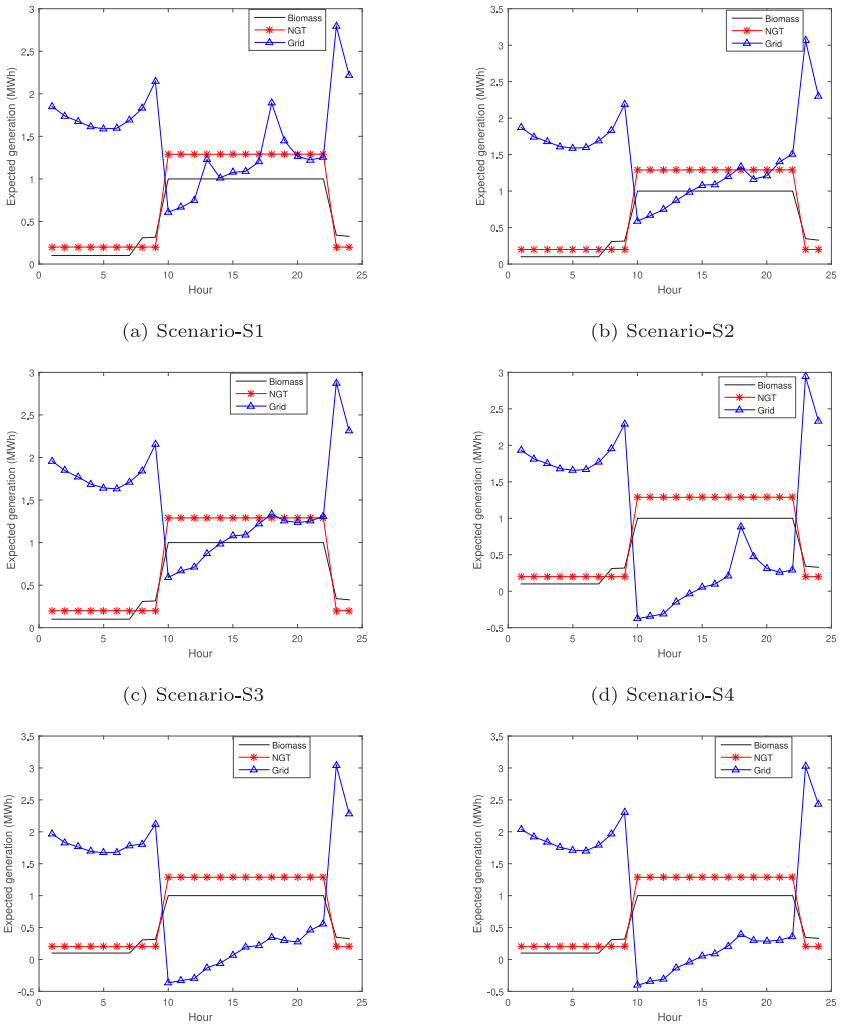

Fig. 5. Expected generation in different scenarios.

dispatchable units produce more power during the peak period. The microgrid also sells power to the main grid during the peak period (see Table 6).

5.4. Impact of optimal scheduling of BESS

Optimal scheduling of BESS further reduces the expected TOC of the system. A coordinated control of BESS scheduling, ELD, and IBDR is implemented in scenarios S7,S8, and S9. The optimal battery schedule for uncoordinated, coordinated, and smart charging strategies are shown in Figs. 8a, 8b, and 8c respectively. The BESS charges during the valley period, while it discharges during the peak period. The grid energy price is low during the valley and off-peak periods. The grid energy price increases during the peak period. The BESS stores energy using inexpensive grid power during the valley period. The stored energy is discharged to supply the load during the peak period. Therefore, optimal scheduling of the BESS provides an arbitrage benefit.

5.5. Impact of ST on voltage, cost and loss

Expected VDM values for scenarios S7, S8, and S9 are shown in Fig. 10. Expected VDMs are negative for hours 8, 9, 23, and 24 with uncoordinated charging (Fig. 10a). In other words, for these hours, the expected minimum voltages of the system become lower than the minimum allowable value of 0.95 pu. Similarly, for coordinated charging strategy, the expected VDM values are negative for hours 9, 23, and 24 (Fig. 10b). The expected VDM values are negative for hours 1, 10, 11, 23, and 24. There is no voltage rise issue above the upper allowable threshold of 1.05 pu in any of the scenarios. Expected power generations for scenarios S7, S8, and S9 are shown in Fig. 9.

A voltage control algorithm is implemented to find the optimal setpoints of the smart transformer to improve the voltage profile of the network. The objective is to minimize the expected average voltage deviation (AVD). The hourly optimal setpoints for the ST for different charging strategies are shown in Table 7. The optimal setpoints of the ST (V^{*}_{STMV}) are more than 1.0 pu for all charging strategies. This is because the system does not suffer from a voltage rise problem, but a voltage drop issue is observed at certain times. Expected VDMs improve and become positive for all hours (see Fig. 10). In other words, the voltage drop problem has been mitigated for all three charging strategies. Expected AVDs for different charging schemes without and with the optimal voltage control strategies are shown in Fig. 11. Expected AVDs reduce for all three charging strategies when optimal voltage control of the ST is implemented. In other words, the system voltage profile will improve considerably when the proposed voltage control scheme is implemented with the ST.

Expected costs and losses are provided in Table 7. The expected TOC is $13 072.11 in scenario S10. Therefore, there is a reduction in expected TOC by ~0.11% compared to scenario S7 (uncoordinated

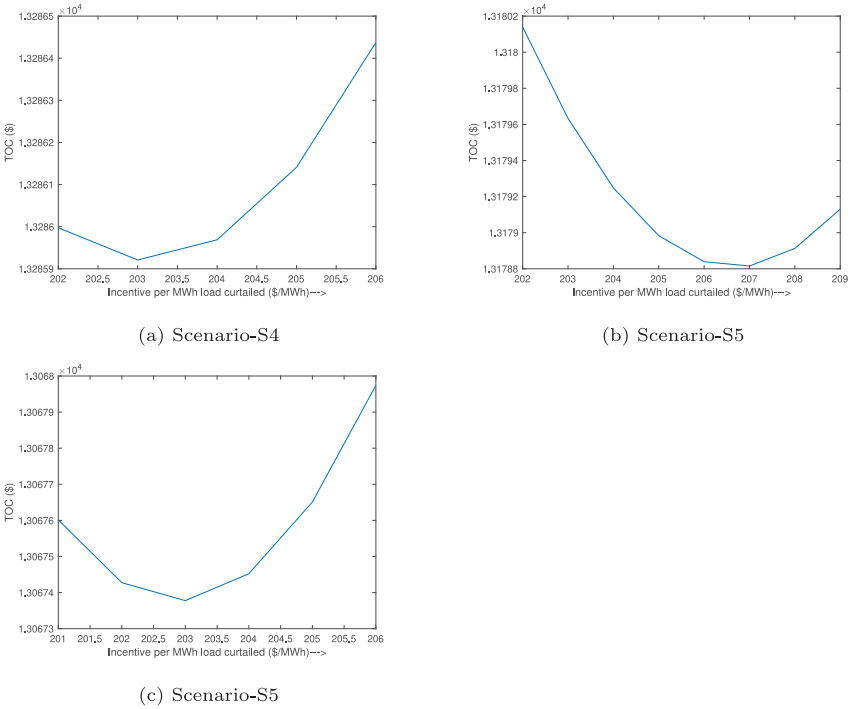

(a) Scenario-S4 (b) Scenario-S5

(c) Scenario-S5

Fig. 6. Variation of TOC with incentive value.

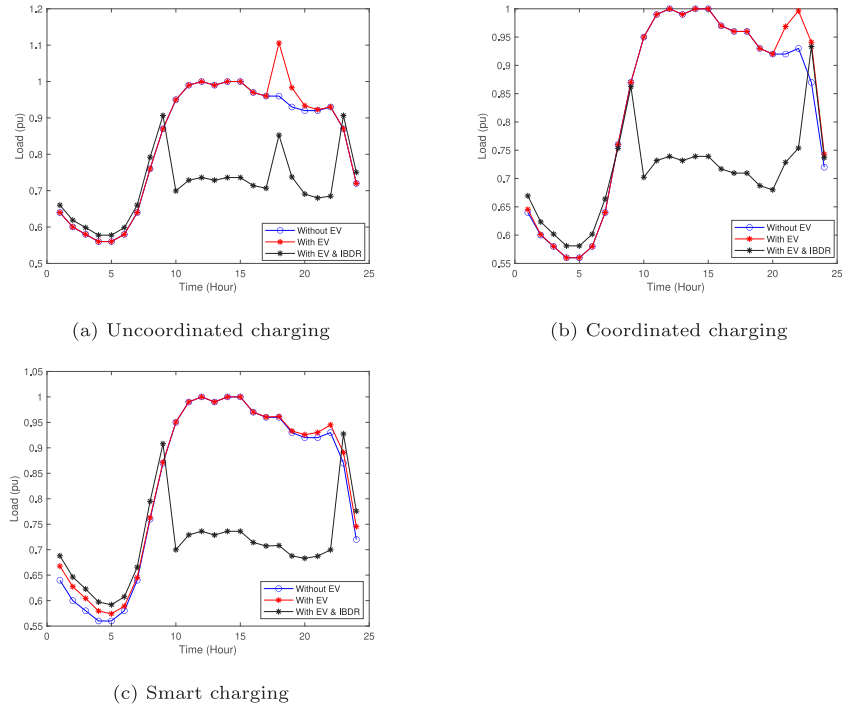

(a) Uncoordinated charging (b) Coordinated charging

(c) Smart charging

Fig. 7. Expected load profiles for different scenarios.

charging strategy). For scenario S11, the expected operating cost is $12 966.28. Therefore, compared to scenario S8, there is a reduction in expected TOC by ~0.10%. The expected TOC is $12 855.45 in scenario S12. Therefore, the expected TOC is 0.06% lower than in scenario S9.

Therefore, there is an incidental reduction in the expected TOC when the voltage control scheme of the ST is implemented. The improvement in the voltage profile also leads to a reduction in network loss. For instance, the expected power loss in scenario S10 is 1444.42 kWh, which is 4.49% lower compared to scenario S7 (uncoordinated charging). Similarly, for scenarios S11 (coordinated charging) and S12 (smart charging), expected losses reduce by 4.37% and 4.44% respectively.

5.6. Convergence characteristics and effect of computational parameters

The convergence characteristic of the PSO algorithm for scenario S1 (hour #24) is shown in Fig. 12a. Convergence characteristics of the PSO

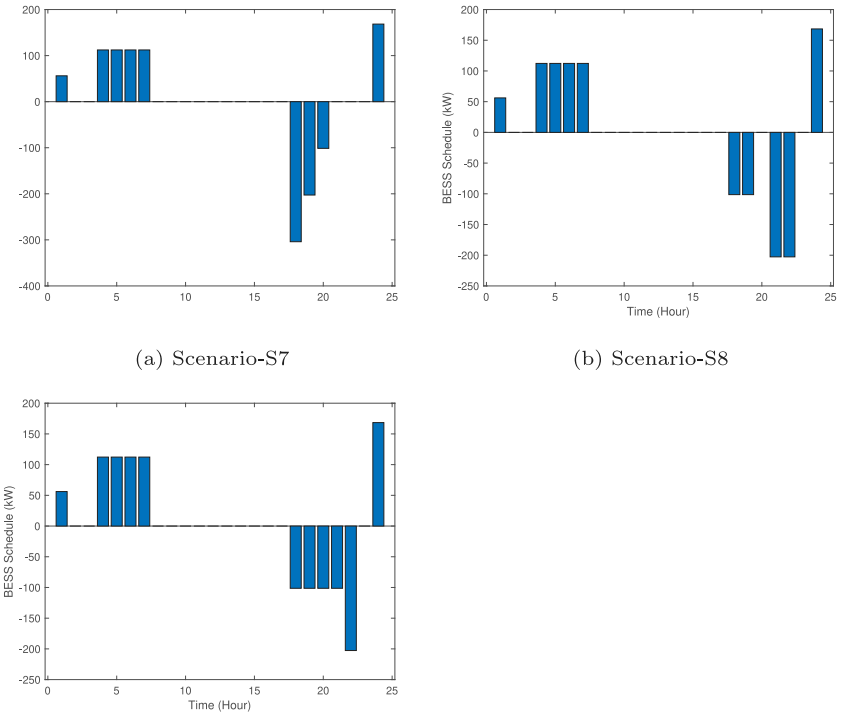

(a) Scenario-S7 (b) Scenario-S8

(c) Scenario-S9

Fig. 8. Optimal battery schedule.

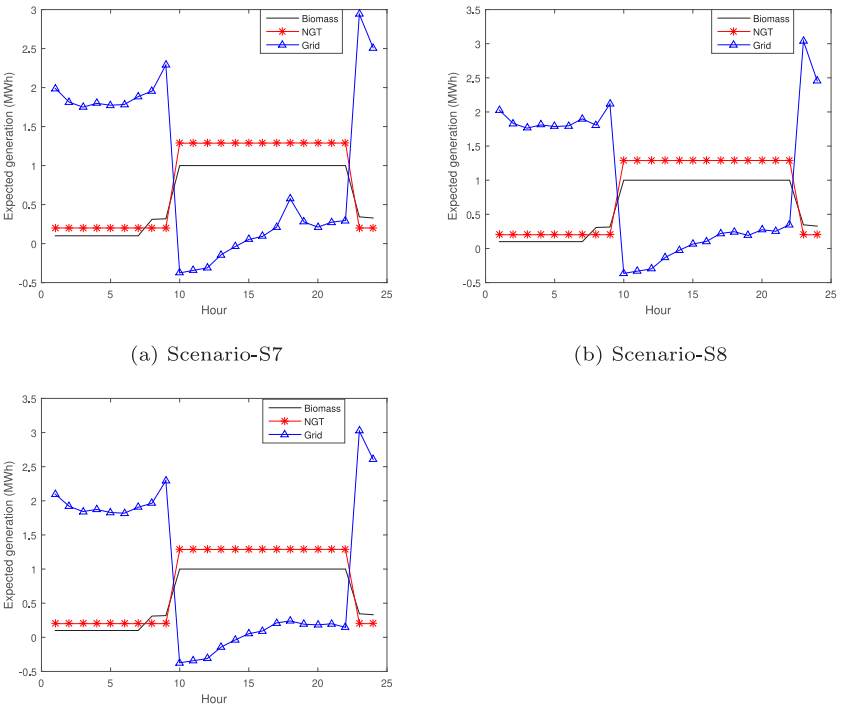

(a) Scenario-S7 (b) Scenario-S8

(c) Scenario-S9

Fig. 9. Expected power generation under different scenarios.

for scenarios S2 and S3 (hour #24 in both cases) are shown in Figs. 12b and Fig. 12c respectively. The objective is to minimize the expected cost. Since the PSO program is formulated as a fitness maximization problem, the fitness value is set to the negative of the expected cost. It is observed from Fig. 12 that the PSO algorithm converges within 10 iterations. The maximum iteration count in the PSO algorithm has been set to 60. Therefore, the PSO algorithm converges much before the maximum iteration count is reached.

The sensitivity of the model with the variation of computational parameters has also been checked. PSO parameters have been varied

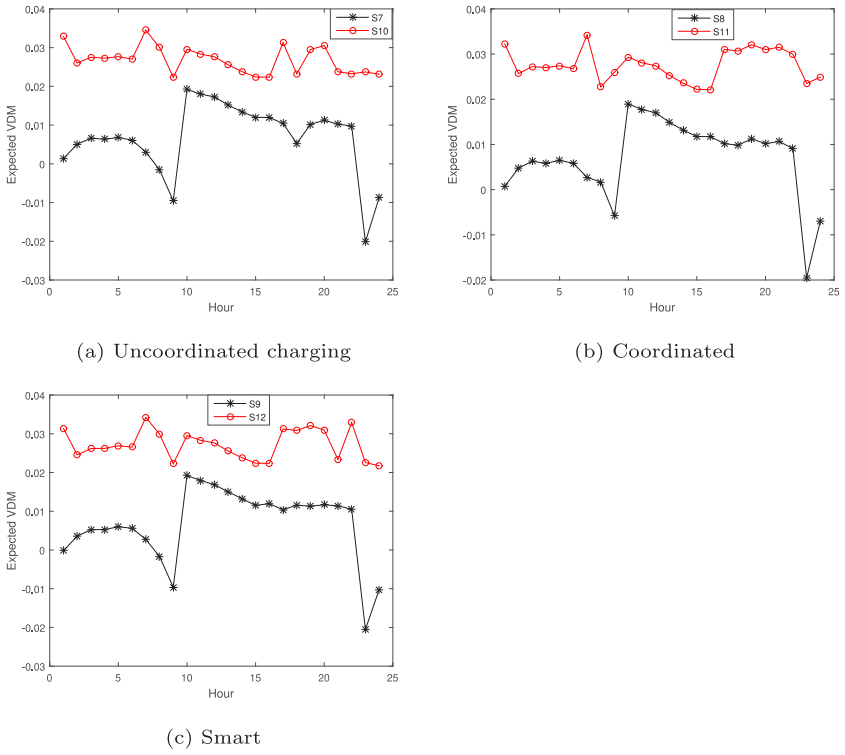

(a) Uncoordinated charging (b) Coordinated

(c) Smart

Fig. 10. Expected VDM under different scenarios.

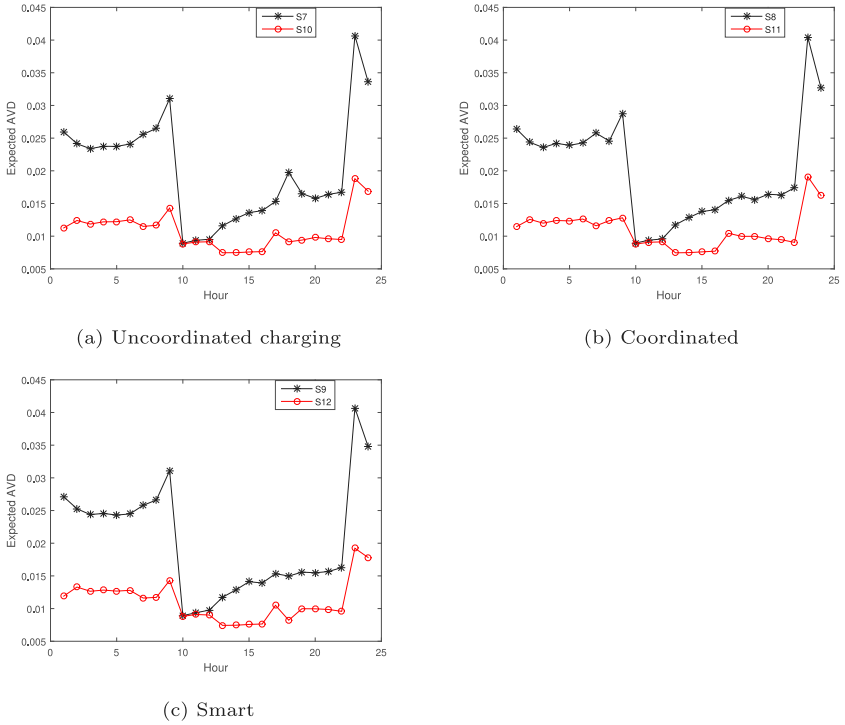

(a) Uncoordinated charging (b) Coordinated

(c) Smart

Fig. 11. Expected AVD under different scenarios.

to find impacts on optimum solutions. The sensitivity of the model with variation in PSO parameters is shown in Table 10. The analysis is carried out for scenario S1, hour #24. Following studies are carried out:

- *Impact of varying the population size:* Trust parameters are set to $c_1 = c_2 = 2.0$, and the maximum iteration count is set to 60. Optimum results for population sizes of 20, 40, and 60 are shown in Table 10. It is observed (see Table 10) that the optimal solution remains unaffected by population sizes ranging between 20 and 60. In most PSO algorithms, the population size is selected between 10 and 20 times the number of control variables.
- *Impact of varying trust parameters:* The population size is set to 40. The maximum iteration is set to 60. Three sets of trust parameters have been used. Set-1: $c_1 = 2.0$, $C_2 = 2.0$; Set-2: $c_1 = 1.5$,

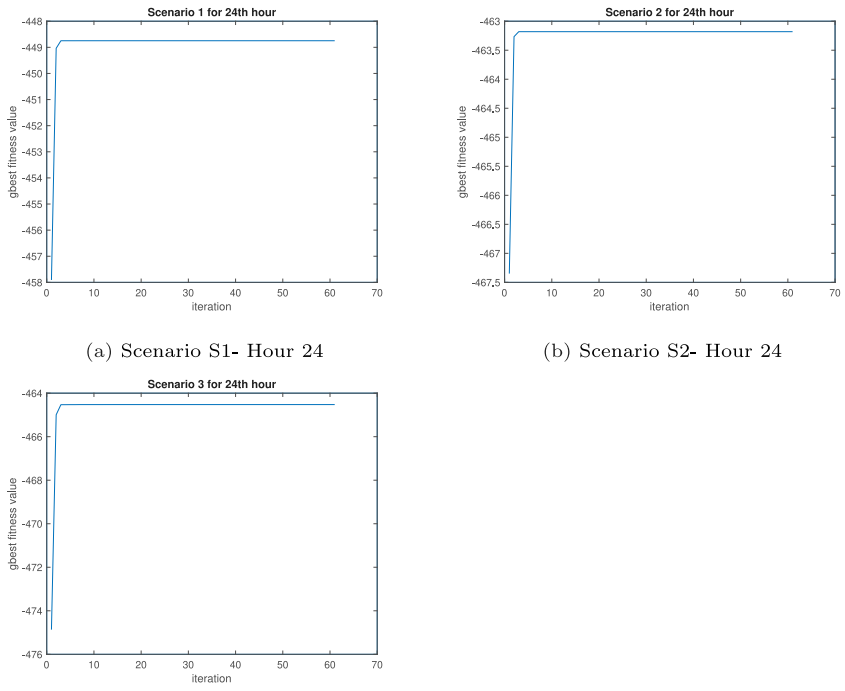

(a) Scenario S1- Hour 24

(b) Scenario S2- Hour 24

(c) Scenario S3- Hour 24

Fig. 12. Convergence characteristics of PSO.

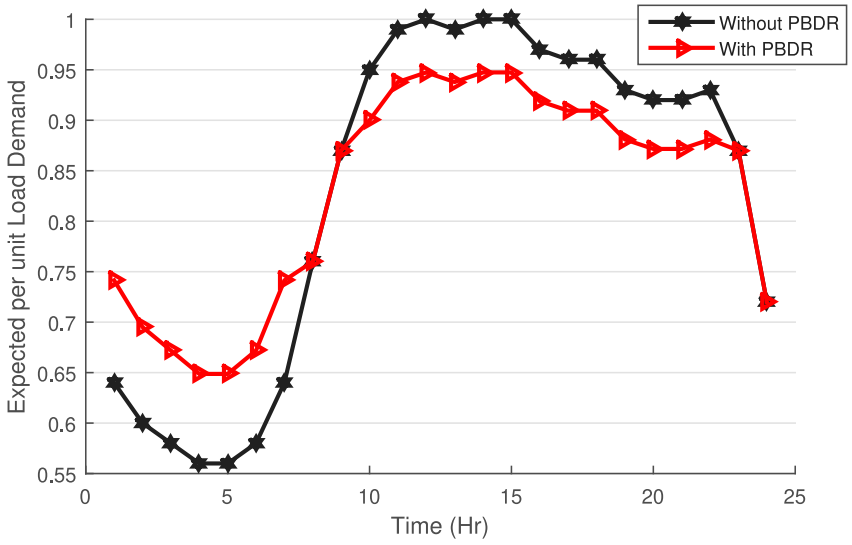

Fig. 13. Load profile with PBDR.

$c_2 = 2.5$; Set-3: $c_1 = 2.5$, $c_2 = 1.5$. It is observed from Table 10 that the optimal solution does not change significantly when trust parameters are varied in close vicinity of standard values.

- *Impact of varying the maximum iteration:* The population size is taken as 40. Trust parameters are set to : $c_1 = c_2 = 2.0$. Optimal values for three different population sizes (20, 40, 60) are tabulated in Table 10. It is seen that the optimal solution is relatively unaffected by maximum iteration counts between 20 and 60. The PSO algorithm converges within 10 iterations (see Fig. 12). Therefore, the optimal solution remains unaffected when the maximum iteration is more than 10.

The above study reveals that the proposed energy management strategy is robust and relatively insensitive to variation of computational parameters.

5.7. Implementation of PBDR

The smart PHEV charging strategy is considered. Following scenarios are implemented:

- *S13a (Base Case):* The system performance is assessed without the PBDR program. Dispatchable units are scheduled optimally using an ELD program.
- *S13b:* The system performance is assessed after the implementation of the PBDR program. Dispatchable units are scheduled optimally using an ELD program.
- *S13c:* The system performance is assessed with an optimal PBDR program, economic scheduling of dispatchable units, and optimal battery dispatch.

Table 8
Expected cost and profits with PBDR.

Hour	S 13a		S 13b		S 13c		S 13d	
	Expected values							
	Cost of energy ($)	Profit ($)	Cost of energy ($)	Profit ($)	Cost of energy ($)	Profit ($)	Cost of energy ($)	Profit ($)
1	136	856.32	434.3	708.67	408.9199	734.06	408.1074	734.87
2	131.5	800.93	146.4	766.21	146.4342	766.21	146.2296	766.42
3	128.5	769.7	142.9	736.61	147.603	731.92	147.397	732.12
4	125.1	736.1	139	705.05	143.715	700.36	143.5325	700.54
5	123.3	729.77	137.2	699.95	146.6043	690.57	146.4068	690.77
6	122.8	752.66	137.3	723	146.6197	713.63	146.4168	713.84
7	126	833.01	394.3	715.42	394.2929	715.42	393.5076	716.2
8	386.2	747.39	386.2	747.46	386.1577	747.46	385.41	748.2
9	437.2	857.65	437.2	857.65	437.2027	857.65	436.0777	858.77
10	792.5	620.13	441.7	896.58	441.7147	896.58	440.4806	897.81
11	822.1	649.38	740.6	723.19	740.5873	723.19	739.5252	724.25
12	839.2	646.92	756.8	721.55	756.8241	721.55	755.7053	722.66
13	904.4	566.81	902.7	560.72	819.0023	644.46	816.741	646.72
14	976	510.09	867.7	610.62	867.6588	610.62	865.8685	612.41
15	988.8	497.36	905.6	572.77	905.5856	572.77	903.6516	574.71
16	992.6	449.2	911.8	522.32	911.8318	522.32	909.9553	524.2
17	1036.4	391.1	983	437.12	899.0123	521.07	896.8993	523.18
18	1124.8	303.98	1010.4	411.04	926.5577	494.87	924.5863	496.84
19	1059.3	327.39	553	760.8	553.0394	760.8	550.8548	762.99
20	1050.2	325.73	550.1	753.85	550.1412	753.85	547.8157	756.18
21	1057	325.04	552.6	757.47	552.5932	757.47	550.5278	759.54
22	1081.7	322.81	562.4	769.35	562.3735	769.35	560.2141	771.51
23	559.1	764.42	558.8	764.79	558.7511	764.79	556.4929	767.05
24	465.2	642.26	465.2	642.26	493.6469	613.81	492.286	615.17
Total	**15 465.9**	**14 426.13**	**13 117.2**	**16 564.44**	**12 896.87**	**16 784.78**	**12 864.69**	**16 816.96**

* S 13a is base case (without PBDR)
* S 13b is for PBDR without battery.
* S 13c is for PBDR with battery.
* S 13d is for PBDR with battery and smart transformer.

- *S13d:* In addition to the measures mentioned in S13c, an optimal voltage control strategy is implemented on the ST to minimize the expected AVD.

The optimal price response is 105% for the peak period and 85% for the valley period. The modified load profile after implementation of the PBDR is shown in Fig. 13. It is observed that a portion of the load demand is shifted from the peak period to the valley period. The load profile remains unchanged in the valley period.

Simulation results are presented in Table 8. The daily expected energy cost (grid energy cost plus fuel cost) in scenario S13a is $15 465.9, while the profit is $14 426.13. The energy cost becomes $13 117.2 (reduces by ~15.19%) when the PBDR is implemented (scenario S13b), while the profit increases to $16 564.44 (an increase by ~14.82%). Optimal scheduling of the BESS (scenario S13c) reduces the expected daily energy cost to $12 896.87, i.e., a reduction of ~16.61%. On the other hand, the expected daily profit becomes $16 784.78 (an increase by ~16.35%). The increase in profit is due to the arbitrage benefit of the battery. In scenario S13d, an optimal voltage control strategy is implemented to minimize the expected hourly AVD. With the improvement of the voltage profile, the loss in the network reduces. As a consequence, the energy drawn from the grid is reduced, leading to a lower expense for purchasing grid energy. Therefore, the profit becomes $16 816.96 (increases by ~16.57%). The energy cost in this scenario is $12 864.69 (a reduction by ~16.82%). Expected AVD, VDM, VRM, and loss for different scenarios are shown in Fig. 14. The voltage profile improves considerably with the implementation of the proposed voltage control strategy in the ST.

The expected energy loss in a day increases by ~8.97% on implementation of the PBDR (see Table 9). The increased loss is due to redistribution of the load over time horizons. The expected energy loss increases further (~9.50% compared to S13a) when the optimal BESS scheduling is considered. A considerable reduction in energy loss compared to scenarios S13b and S13c is achieved on implementation of the optimal voltage control strategy (scenario S13d). The loss is only ~1.67% more compared to scenario S13a. In other words, the expected energy loss reduces by ~7.15% compared to scenario S13c with the optimal voltage control strategy. Although daily expected energy losses increase in scenarios S13b and S13c, expected profits in the two scenarios are higher than that in scenario S13a.

Table 9
Results for PBDR.

Comparison w.r.t S13a			
Scenarios	Expected cost of energy (%)	Expected profit (%)	Expected loss (%)
S13b	−15.19	14.82	8.97
S13c	−16.61	16.35	9.5
S13d	−16.82	16.57	1.67

Negative : Reduction; Positive: Increase.

5.8. Comparison with other methods

The proposed method has been compared with the energy management scheme suggested in [90]. Comparison results are given in Table 11. The reduction in fuel and energy purchase cost is ~10.62% on implementing the DRP proposed in [90]. Simultaneous implementation of the DRP and network reconfiguration reduces the cost by ~11.97% [90]. On the other hand, with the proposed method, the reduction in the expected TOC is ~16.19% in scenario S4 (uncoordinated PHEV charging). The expected savings are ~17.45% and

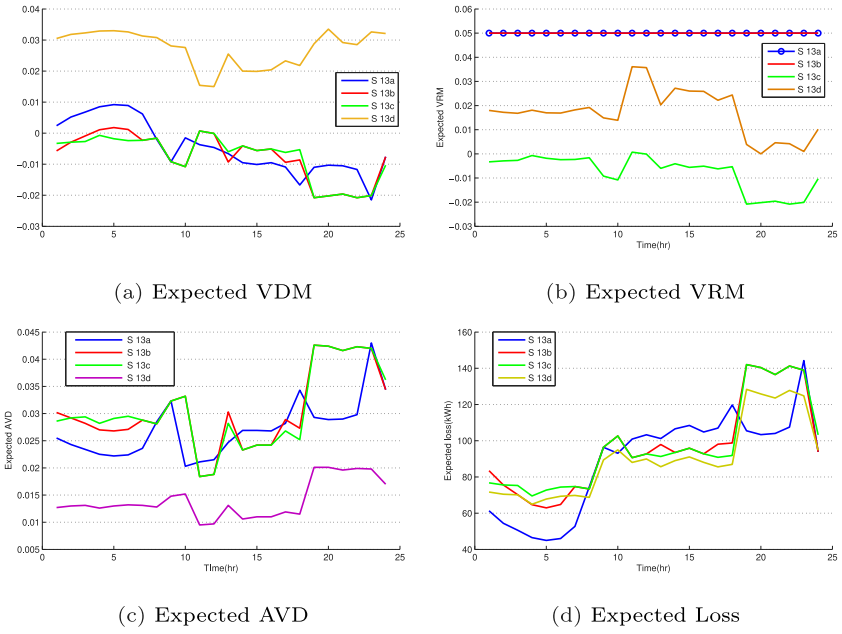

(a) Expected VDM (b) Expected VRM

(c) Expected AVD (d) Expected Loss

Fig. 14. Performance indices with PBDR-smart PHEV charging.

Table 10
Sensitivity of the model with variation of computational parameters.

Variation with population size ($c_1 = c_2 = 2.0$; Maxm Iter = 40)		Variation with trust parameters (Population size = 40; Maxm Iter = 60)		Variation with maximum iteration ($c_1 = c_2 = 2.0$; Population Size = 40)	
Population size	Expected cost	c_1, c_2	Expected cost	Maxm iteration	Expected cost
20	448.75	$c_1 = 2$; $c_2 = 2.0$	448.75	20	448.75
40	448.75	$c_1 = 1.5$; $c_2 = 2.5$	448.75	40	448.75
60	448.75	$c_1 = 2.5$; $c_2 = 1.5$	448.75	60	448.75

Table 11
Comparison with [90].

Proposed method			
PHEV charging strategy	Reduction in expected TOC (%)		
Uncoordinated	S4 w.r.t S1 16.19	S7 w.r.t S1 17.45	S10 w.r.t S1 17.54
Coordinated	S5 w.r.t S2 16.36	S8 w.r.t S2 17.63	S11 w.r.t S2 17.71
Smart	S6 w.r.t S3 16.38	S9 w.r.t S3 17.69	S12 w.r.t S3 17.74
Energy management strategy given in [90]			
	Demand response in original network	Demand response in reconfigured network	
Reduction in expected energy cost w.r.t the base case (%)	10.62	11.97	

~17.54% respectively in scenarios S7 and S10 (uncoordinated PHEV charging). With a coordinated PHEV charging, savings are around ~16.36%, ~17.63%, and ~17.71% in scenarios S5, S8, and S11, respectively. With a smart charging strategy, reductions in expected TOCs are ~16.38%, ~17.69%, and ~17.74% in scenarios S6, S9, and S12, respectively. Therefore, expected savings using the proposed energy management scheme is 16.19%~17.74% as opposed to 10.62%~11.97% obtained in [90].

6. Conclusions

A stochastic coordinated energy management system has been proposed for a grid-connected microgrid. Uncertainties of load, renewable generation, PHEVs, grid energy power price have been modeled using the "Hong's 2 m PEM" approach. A detailed algorithm for stochastic modeling PHEV load for three different charging strategies has been proposed. The battery charging characteristic has been taken into account while carrying out the stochastic modeling of the PHEV load. Proper coordination between a group of energy management measures like ELD, BESS scheduling, and IBDR has been proposed to obtain optimal economic performance. The incentive value of the IBDR scheme is also optimized for different PHEV charging strategies. Moreover, the use of ST is proposed and integrated with the stochastic energy management scheme to improve the voltage profile of the network and reduce network loss. The optimal voltage control strategy implemented with the ST also leads to an incidental reduction in the expected TOC. The proposed method is validated by simulation studies on a thirty-three bus system. The expected TOC is the least for the smart charging strategy. The expected TOC can be reduced to the tune of 16.19%~16.38% with an optimally designed IBDR program. The reduction in expected cost is about 17.45%~17.69% with optimal coordination between ELD, IBDR, and BESS scheduling. The ST improves the system profile and reduces network loss. The ST also slightly reduces the system loss. The network loss can be reduced by about 29.49%~31.36% by optimal coordination between the voltage control strategy, ELD, IBDR, and BESS scheduling. An optimal PBDR strategy is also coordinated with the energy management scheme. The implementation of the PBDR increases the expected daily profit by ~16.57% and reduces the expected daily energy cost by ~16.82%

A balanced three-phase network has been considered in this work. The proposed EMS framework may be adopted with suitable changes for an unbalanced network in a future job. Also, probabilistic correlations between wind and solar generation, conventional loads, and EV demands may be incorporated in the EMS framework in the future.

CRediT authorship contribution statement

S. Gupta: Software, Validation. **A. Maulik:** Conceptualization, Methodology, Software, validation, Writing – original draft. **D. Das:** Supervision. **A. Singh:** Rewriting, Draft preparation during revision.

Declaration of competing interest

The authors declare that they have no known competing financial interests or personal relationships that could have appeared to influence the work reported in this paper.

References

[1] Ackermann T, Andersson G, Söder L. Distributed generation: a definition. Electr Power Syst Res 2001;57(3):195–204.
[2] Lasseter RH, Paigi P. Microgrid: A conceptual solution. In: 2004 ieee 35th annual power electronics specialists conference (ieee cat. no. 04ch37551), Vol. 6. IEEE; 2004, p. 4285–90.
[3] Imani MH, Ghadi MJ, Ghavidel S, Li L. Demand response modeling in microgrid operation: a review and application for incentive-based and time-based programs. Renew Sustain Energy Rev 2018;94:486–99.
[4] Zeynali S, Rostami N, Ahmadian A, Elkamel A. Two-stage stochastic home energy management strategy considering electric vehicle and battery energy storage system: An ann-based scenario generation methodology. Sustain Energy Technol Assess 2020;39:100722.
[5] Aliasghari P, Mohammadi-Ivatloo B, Alipour M, Abapour M, Zare K. Optimal scheduling of plug-in electric vehicles and renewable micro-grid in energy and reserve markets considering demand response program. J Cleaner Prod 2018;186:293–303.
[6] Yang J, Liu J, Fang Z, Liu W. Electricity scheduling strategy for home energy management system with renewable energy and battery storage: a case study. IET Renew Power Gener 2018;12(6):639–48.
[7] Gazijahani FS, Salehi J. Reliability constrained two-stage optimization of multiple renewable-based microgrids incorporating critical energy peak pricing demand response program using robust optimization approach. Energy 2018;161:999–1015.
[8] Noor S, Yang W, Guo M, van Dam KH, Wang X. Energy demand side management within micro-grid networks enhanced by blockchain. Appl Energy 2018;228:1385–98.
[9] Müller T, Möst D. Demand response potential: available when needed? Energy Policy 2018;115:181–98.
[10] Nan S, Zhou M, Li G. Optimal residential community demand response scheduling in smart grid. Appl Energy 2018;210:1280–9.
[11] Pfeifer A, Dobravec V, Pavlinek L, Krajačić G, Duić N. Integration of renewable energy and demand response technologies in interconnected energy systems. Energy 2018;161:447–55.
[12] Gazijahani FS, Salehi J. Integrated dr and reconfiguration scheduling for optimal operation of microgrids using hong's point estimate method. Int J Electr Power Energy Syst 2018;99:481–92.
[13] Imani MH, Yousefpour K, Andani MT, Ghadi MJ. Effect of changes in incentives and penalties on interruptible/curtailable demand response program in microgrid operation. In: 2019 ieee texas power and energy conference (tpec). IEEE; 2019, p. 1–6.
[14] Biroon RA, Hadidi R, Abdollahi Z. On the tariff modification for the future electric vehicle connection to the grid. In: 2019 north american power symposium (naps). IEEE; 2019, p. 1–6.
[15] Zhou Z, Wang B, Guo Y, Zhang Y. Blockchain and computational intelligence inspired incentive-compatible demand response in internet of electric vehicles. IEEE Transactions on Emerging Topics in Computational Intelligence 2019;3(3):205–16.
[16] Monfared HJ, Ghasemi A, Loni A, Marzband M. A hybrid price-based demand response program for the residential micro-grid. Energy 2019;185:274–85.
[17] Good N. Using behavioural economic theory in modelling of demand response. Appl Energy 2019;239:107–16.
[18] Khalili T, Jafari A, Abapour M, Mohammadi-Ivatloo B. Optimal battery technology selection and incentive-based demand response program utilization for reliability improvement of an insular microgrid. Energy 2019;169:92–104.
[19] Eseye AT, Lehtonen M, Tukia T, Uimonen S, Millar RJ. Optimal energy trading for renewable energy integrated building microgrids containing electric vehicles and energy storage batteries. IEEE Access 2019;7:106092–101.
[20] Li Y, Li K. Incorporating demand response of electric vehicles in scheduling of isolated microgrids with renewables using a bi-level programming approach. IEEE Access 2019;7:116256–66.
[21] Sadeghian O, Nazari-Heris M, Abapour M, Taheri SS, Zare K. Improving reliability of distribution networks using plug-in electric vehicles and demand response. J Mod Power Syst Clean Energy 2019;7(5):1189–99.
[22] Iwafune Y, Ogimoto K, Kobayashi Y, Murai K. Driving simulator for electric vehicles using the markov chain monte carlo method and evaluation of the demand response effect in residential houses. IEEE Access 2020;8:47654–63.
[23] Ren H, Zhang A, Wang F, Yan X, Li Y, Duić N, Shafie-khah M, Catalão JP. Optimal scheduling of an ev aggregator for demand response considering triple level benefits of three-parties. Int J Electr Power Energy Syst 2021;125:106447.
[24] Gao J, Yang Y, Ma Z, Gao F. Ggluevar-based participation of electric vehicles in automatic demand response for two-stage scheduling. Int J Energy Res 2021;45(1):1128–41.
[25] Wang X, Pei L, Zheng S, Wang W. Optimal scheduling mechanism for ev charging and discharging with multi-price scales and comprehensive demand. In: 2021 ieee asia-pacific conference on image processing, electronics and computers (ipec). IEEE; 2021, p. 711–5.
[26] Yusuf J, Hasan AJ, Ula S. Impacts analysis & field implementation of plug-in electric vehicles participation in demand response and critical peak pricing for commercial buildings. In: 2021 ieee texas power and energy conference (tpec). IEEE; 2021, p. 1–6.
[27] Qian K, Zhou C, Allan M, Yuan Y. Modeling of load demand due to ev battery charging in distribution systems. IEEE Trans Power Syst 2010;26(2):802–10.
[28] Shaaban MF, Atwa YM, El-Saadany EF. Pevs modeling and impacts mitigation in distribution networks. IEEE Trans Power Syst 2012;28(2):1122–31.
[29] Mu Y, Wu J, Jenkins N, Jia H, Wang C. A spatial–temporal model for grid impact analysis of plug-in electric vehicles. Appl Energy 2014;114:456–65.
[30] Honarmand M, Zakariazadeh A, Jadid S. Integrated scheduling of renewable generation and electric vehicles parking lot in a smart microgrid. Energy Convers Manage 2014;86:745–55.
[31] Rostami M-A, Kavousi-Fard A, Niknam T. Expected cost minimization of smart grids with plug-in hybrid electric vehicles using optimal distribution feeder reconfiguration. IEEE Trans Ind Inf 2015;11(2):388–97.
[32] Yao L, Lim WH, Tsai TS. A real-time charging scheme for demand response in electric vehicle parking station. IEEE Trans Smart Grid 2016;8(1):52–62.
[33] Kamankesh H, Agelidis VG, Kavousi-Fard A. Optimal scheduling of renewable micro-grids considering plug-in hybrid electric vehicle charging demand. Energy 2016;100:285–97.
[34] Chaudhari K, Ukil A, Kumar KN, Manandhar U, Kollimalla SK. Hybrid optimization for economic deployment of ess in pv-integrated ev charging stations. IEEE Trans Ind Inf 2017;14(1):106–16.
[35] Rahmani-Andebili M, Fotuhi-Firuzabad M. An adaptive approach for pevs charging management and reconfiguration of electrical distribution system penetrated by renewables. IEEE Trans Ind Inf 2017;14(5):2001–10.
[36] Quddus MA, Shahvari O, Marufuzzaman M, Usher JM, Jaradat R. A collaborative energy sharing optimization model among electric vehicle charging stations, commercial buildings, and power grid. Appl Energy 2018;229:841–57.
[37] Moghaddas-Tafreshi SM, Jafari M, Mohseni S, Kelly S. Optimal operation of an energy hub considering the uncertainty associated with the power consumption of plug-in hybrid electric vehicles using information gap decision theory. Int J Electr Power Energy Syst 2019;112:92–108.
[38] Emrani-Rahaghi P, Hashemi-Dezaki H. Optimal scenario-based operation and scheduling of residential energy hubs including plug-in hybrid electric vehicle and heat storage system considering the uncertainties of electricity price and renewable distributed generations. J Energy Storage 2021;33:102038.
[39] Ahrabi M, Abedi M, Nafisi H, Mirzaei MA, Mohammadi-Ivatloo B, Marzband M. Evaluating the effect of electric vehicle parking lots in transmission-constrained ac unit commitment under a hybrid igdt-stochastic approach. Int J Electr Power Energy Syst 2021;125:106546.
[40] Lan T, Liu X, Wang S, Jermsittiparsert K, Alrashood ST, Rezaei M, Al-Ghussain L, Mohamed MA. An advanced machine learning based energy management of renewable microgrids considering hybrid electric vehicles' charging demand. Energies 2021;14(3):569.
[41] Mohamed MA, Jin T, Su W. Multi-agent energy management of smart islands using primal-dual method of multipliers. Energy 2020;208:118306.
[42] Ma H, Liu Z, Li M, Wang B, Si Y, Yang Y, Mohamed MA. A two-stage optimal scheduling method for active distribution networks considering uncertainty risk. Energy Rep 2021;7:4633–41.
[43] Mohamed MA, Abdullah HM, El-Meligy MA, Sharaf M, Soliman AT, Hajjiah A. A novel fuzzy cloud stochastic framework for energy management of renewable microgrids based on maximum deployment of electric vehicles. Int J Electr Power Energy Syst 2021;129:106845.
[44] Li Y, Han M, Yang Z, Li G. Coordinating flexible demand response and renewable uncertainties for scheduling of community integrated energy systems with an electric vehicle charging station: A bi-level approach. IEEE Trans Sustain Energy 2021.
[45] Alfaverh F, Denai M, Sun Y. Electrical vehicle grid integration for demand response in distribution networks using reinforcement learning. IET Electr Syst Transp 2021.

[46] Ghofrani M, Majidi M. A comprehensive optimization framework for ev-renewable dg coordination. Electr Power Syst Res 2021;194:107086.
[47] Liserre M, Buticchi G, Andresen M, De Carne G, Costa LF, Zou Z-X. The smart transformer: Impact on the electric grid and technology challenges. IEEE Ind Electron Mag 2016;10(2):46–58.
[48] Vandoorn TL, De Kooning JD, Meersman B, Guerrero JM, Vandevelde L. Voltage-based control of a smart transformer in a microgrid. IEEE Trans Ind Electron 2011;60(4):1291–305.
[49] De Carne G, Liserre M, Christakou K, Paolone M. Integrated voltage control and line congestion management in active distribution networks by means of smart transformers. In: 2014 ieee 23rd international symposium on industrial electronics (isie). IEEE; 2014, p. 2613–9.
[50] Watson JD, Watson NR, Das B. Effectiveness of power electronic voltage regulators in the distribution network. IET Gener Transm Distrib 2016;10(15):3816–23.
[51] Hrishikesan V, Das D, Kumar C. A flexible and coordinated voltage control strategy for smart transformer. In: 2018 ieee international conference on power electronics, drives and energy systems (pedes). IEEE; 2018, p. 1–6.
[52] Zhu R, Zou Z, Liserre M. High power quality voltage control of smart transformer-fed distribution grid. In: Iecon 2018-44th annual conference of the ieee industrial electronics society. IEEE; 2018, p. 5547–52.
[53] Manojkumar R, Hrishikesan V, Kumar C, Ganguly S. Voltage control using smart transformer for increasing photovoltaic penetration in a distribution grid. In: 2019 20th international conference on intelligent system application to power systems (isap). IEEE; 2019, p. 1–7.
[54] Willems W, Vandoorn TL, De Kooning JD, Vandevelde L. Development of a smart transformer to control the power exchange of a microgrid. In: Ieee pes isgt europe 2013. IEEE; 2013, p. 1–5.
[55] VC JS, Haritha G, Nair MG. Smart transformer based power flow control in multi microgrid system. In: 2016 international conference on energy efficient technologies for sustainability (iceets). IEEE; 2016, p. 366–71.
[56] Couto M, Lopes JP, Moreira C. Control strategies for multi-microgrids islanding operation through smart transformers. Electr Power Syst Res 2019;174:105866.
[57] Chen J, Liu M, De Carne G, Zhu R, Liserre M, Milano F, O'Donnell T. Impact of smart transformer voltage and frequency support in a high renewable penetration system. Electr Power Syst Res 2021;190:106836.
[58] Wang P, Wang D, Zhu C, Yang Y, Abdullah HM, Mohamed MA. Stochastic management of hybrid ac/dc microgrids considering electric vehicles charging demands. Energy Rep 2020;6:1338–52.
[59] Xia T, Rezaei M, Dampage U, Alharbi SA, Nasif O, Borowski PF, Mohamed MA. Techno-economic assessment of a grid-independent hybrid power plant for co-supplying a remote micro-community with electricity and hydrogen. Processes 2021;9(8):1375.
[60] Singh A, Maulik A, Das D. Stochastic impact assessment of phev charger levels in a microgrid. In: 2021 innovations in energy management and renewable resources (52042). IEEE; 2021, p. 1–6.
[61] Soroudi A, Amraee T. Decision making under uncertainty in energy systems: State of the art. Renew Sustain Energy Rev 2013;28:376–84.
[62] Hasan KN, Preece R, Milanović JV. Existing approaches and trends in uncertainty modelling and probabilistic stability analysis of power systems with renewable generation. Renew Sustain Energy Rev 2019;101:168–80.
[63] Hong H. An efficient point estimate method for probabilistic analysis. Reliab Eng Syst Saf 1998;59(3):261–7.
[64] Su C-L. Probabilistic load-flow computation using point estimate method. IEEE Trans Power Syst 2005;20(4):1843–51.
[65] Su C-L, Lu C-N. Two-point estimate method for quantifying transfer capability uncertainty. IEEE Trans Power Syst 2005;20(2):573–9.
[66] Hafez O, Bhattacharya K. Integrating ev charging stations as smart loads for demand response provisions in distribution systems. IEEE Trans Smart Grid 2016;9(2):1096–106.
[67] Bett PE, Thornton HE. The climatological relationships between wind and solar energy supply in britain. Renew Energy 2016;87:96–110.
[68] Atwa Y, El-Saadany E, Salama M, Seethapathy R. Optimal renewable resources mix for distribution system energy loss minimization. IEEE Trans Power Syst 2009;25(1):360–70.
[69] Niknam T, Kavousifard A, Aghaei J. Scenario-based multiobjective distribution feeder reconfiguration considering wind power using adaptive modified particle swarm optimisation. IET Renew Power Gener 2012;6(4):236–47.
[70] Al Abri R, El-Saadany EF, Atwa YM. Optimal placement and sizing method to improve the voltage stability margin in a distribution system using distributed generation. IEEE Trans Power Syst 2012;28(1):326–34.
[71] Liu P-L, Der Kiureghian A. Multivariate distribution models with prescribed marginals and covariances. Probab Eng Mech 1986;1(2):105–12.
[72] Andervazh M-R, Javadi S. Emission-economic dispatch of thermal power generation units in the presence of hybrid electric vehicles and correlated wind power plants. IET Gener Transm Distrib 2017;11(9):2232–43.
[73] Jithendranath J, Das D, Guerrero JM. Probabilistic optimal power flow in islanded microgrids with load, wind and solar uncertainties including intermittent generation spatial correlation. Energy 2021;222:119847.
[74] Manojkumar R, Kumar C, Ganguly S, Gooi HB, Mekhilef S. Voltage control using smart transformer via dynamic optimal setpoints and limit tolerance in a residential distribution network with pv sources. IET Gener Transm Distrib 2020;14(22):5143–51.
[75] Gampa SR, Jasthi K, Goli P, Das D, Bansal R. Grasshopper optimization algorithm based two stage fuzzy multiobjective approach for optimum sizing and placement of distributed generations, shunt capacitors and electric vehicle charging stations. J Energy Storage 2020;27:101117.
[76] Aalami H, Moghaddam MP, Yousefi G. Modeling and prioritizing demand response programs in power markets. Electr Power Syst Res 2010;80(4):426–35.
[77] Abdollahi A, Moghaddam MP, Rashidinejad M, Sheikh-El-Eslami MK. Investigation of economic and environmental-driven demand response measures incorporating uc. IEEE Trans Smart Grid 2011;3(1):12–25.
[78] Nayak A, Maulik A, Das D. An integrated optimal operating strategy for a grid-connected ac microgrid under load and renewable generation uncertainty considering demand response. Sustain Energy Technol Assess 2021;45:101169.
[79] Zhang C, Xu Y, Dong ZY, Wong KP. Robust coordination of distributed generation and price-based demand response in microgrids. IEEE Trans Smart Grid 2017;9(5):4236–47.
[80] Tan H, Yan W, Ren Z, Wang Q, Mohamed MA. A robust dispatch model for integrated electricity and heat networks considering price-based integrated demand response. Energy 2021;121875.
[81] Eberhart R, Kennedy J. Particle swarm optimization. In: Proceedings of the ieee international conference on neural networks, Vol. 4. Citeseer; 1995, p. 1942–8.
[82] Kong X, Bai L, Hu Q, Li F, Wang C. Day-ahead optimal scheduling method for grid-connected microgrid based on energy storage control strategy. J Mod Power Syst Clean Energy 2016;4(4):648–58.
[83] Maulik A, Das D. Optimal operation of droop-controlled islanded microgrids. IEEE Trans Sustain Energy 2017;9(3):1337–48.
[84] Das D, Kothari D, Kalam A. Simple and efficient method for load flow solution of radial distribution networks. Int J Electr Power Energy Syst 1995;17(5):335–46.
[85] Baran ME, Wu FF. Network reconfiguration in distribution systems for loss reduction and load balancing. IEEE Power Eng Rev 1989;9(4):101–2.
[86] Kayal P, Chanda C. Optimal mix of solar and wind distributed generations considering performance improvement of electrical distribution network. Renew Energy 2015;75:173–86.
[87] Gelaro R, McCarty W, Suárez MJ, Todling R, Molod A, Takacs L, Randles CA, Darmenov A, Bosilovich MG, Reichle R, et al. The modern-era retrospective analysis for research and applications, version 2 (merra-2). J Clim 2017;30(14):5419–54.
[88] Das B, Mukherjee V, Das D. Optimum dg placement for known power injection from utility/substation by a novel zero bus load flow approach. Energy 2019;175:228–49.
[89] Maulik A, Das D. Optimal operation of a droop-controlled dcmg with generation and load uncertainties. IET Gener Transm Distrib 2018;12(12):2905–17.
[90] Harsh P, Das D. Energy management in microgrid using incentive-based demand response and reconfigured network considering uncertainties in renewable energy sources. Sustain Energy Technol Assess 2021;46:101225.